

# Homogenization of sub-genome secretome gene expression patterns in the allodiploid fungus *Verticillium longisporum*

Jasper R.L. Depotter<sup>1,2</sup>, Fabian van Beveren<sup>1¶</sup>, Luis Rodriguez-Moreno<sup>1¶</sup>, Grady C.M. van den Berg<sup>1</sup>, Thomas A. Wood<sup>2&</sup>, Bart P.H.J. Thomma<sup>1&\*</sup>, Michael F. Seidl<sup>1&\*</sup>

<sup>1</sup>Laboratory of Phytopathology, Wageningen University & Research, Wageningen, The Netherlands

<sup>2</sup>Department of Crops and Agronomy, National Institute of Agricultural Botany, Cambridge, United Kingdom

\*Corresponding authors

E-mail: bart.thomma@wur.nl (BPHJT)

E-mail: michael.seidl@wur.nl (MFS)

¶These authors contributed equally to this work

&These authors also contributed equally to this work

## Abstract

Allopolyploidization, genome duplication through interspecific hybridization, is an important evolutionary mechanism that can enable organisms to adapt to environmental changes or stresses. The increased adaptive potential of allopolyploids can be particularly relevant for plant pathogens in their ongoing quest for host immune response evasion. To this end, plant pathogens secrete a plethora of molecules that enable host colonization. Allodiploidization has resulted in the new plant pathogen *Verticillium longisporum* that infects different hosts than haploid *Verticillium* species. To reveal the impact of allodiploidization on plant pathogen evolution, we studied the genome and transcriptome dynamics of *V. longisporum* using next-generation sequencing. *V. longisporum* genome evolution is characterized by extensive chromosomal rearrangements, between as well as within parental chromosome sets, leading to a mosaic genome structure. In comparison to haploid *Verticillium* species, *V. longisporum* genes display stronger signs of positive selection. The expression patterns of the two sub-genomes show remarkable resemblance, suggesting that the parental gene expression patterns homogenized upon hybridization. Moreover, whereas *V. longisporum* genes encoding secreted proteins frequently display differential expression between the parental sub-genomes in culture medium, expression patterns homogenize upon plant colonization. Collectively, our results illustrate of the adaptive potential of allodiploidy mediated by the interplay of two sub-genomes.

## Author summary

Hybridization followed by whole-genome duplication, so-called allopolyploidization, provides genomic flexibility that is beneficial for survival under stressful conditions or invasiveness into new habitats. Allopolyploidization has mainly been studied in plants, but also occurs in other organisms, including fungi. *Verticillium longisporum*, an emerging fungal pathogen on brassicaceous plants, arose by allodiploidization between two *Verticillium* spp. We used comparative genomics to reveal the plastic nature of the *V. longisporum* genomes, showing that parental chromosome sets recombined extensively, resulting in a mosaic genome pattern. Furthermore, we show that non-synonymous substitutions frequently occurred in *V. longisporum*. Moreover, we reveal that expression patterns of genes encoding secreted proteins homogenized between the *V. longisporum* sub-genomes upon plant colonization. In conclusion, our results illustrate the large adaptive potential upon genome hybridization for fungi mediated by genomic plasticity and interaction between sub-genomes.

## Introduction

Cycles of polyploidization are hallmarks of eukaryotic genome evolution, where an initial increase of ploidy is commonly followed by reversions to original ploidy states [1]. For instance, all angiosperm plants share two rounds of ancient polyploidy [2]. The prevalence of polyploidy events in eukaryotic evolution is likely due to the high evolutionary potential of polyploids, as additional chromosome sets give leeway to functional diversification [3]. Consequently, polyploidy events are often followed by adaptive radiation and are dated near the base of species-rich clades in phylogenies [4,5]. In addition, polyploidy has been associated with increased invasiveness [6] and resistance to environmental stresses [7]. For instance, numerous plant species that survived the Cretaceous-Palaeogene mass extinction 66 million years ago underwent a polyploidization event which is thought to have contributed to their increased survival rates [8,9]. Polyploids may originate from the same species, i.e. autopolyploidization, or from different species as a result of interspecific hybridization, i.e. allopolyploidization. In general, allopolyploids are believed to have a higher adaptive potential than autopolyploids due to the combination of novel or diverged genes from distinct parental species [3].

The impact of allopolyploidization has mainly been investigated in plants, as approximately a tenth of all plant species consists of allopolyploids [10]. In contrast, allopolyploidization in fungi is far less intensively investigated [11]. Nonetheless, allopolyploidization impacted the evolution of numerous fungal species, including the economically important baker's yeast *Saccharomyces cerevisiae* [12]. The increased adaptive potential enabled allopolyploid fungi to develop desirable traits that can be exploited in industrial bioprocessing [13]. For instance, at least two recent hybridization events between *S. cerevisiae* and its close relative *Saccharomyces eubayanus* gave rise to *Saccharomyces pastorianus*, a species with high cold tolerance and good maltose/maltotriose utilization

capabilities, which is exploited in the production of lager beer that requires barley to be malted at low temperatures [14].

Allopolyploid genomes experience a so-called “genome shock” upon hybridization, inciting major genomic reorganizations that can manifest by genome rearrangements, extensive gene loss, transposon activation, and alterations in gene expression [15]. These early stage alterations are primordial for hybrid survival, as divergent evolution is principally associated with incompatibilities between the parental genomes [16]. Additionally, these initial re-organizations and further alterations in the aftermath of hybridization also provide a source for environmental adaptation [3]. Frequently, heterozygosity is lost for many regions in the allopolyploid genome [17]. This can be a result of the direct loss of a homolog of different parental origin (i.e. a homeolog) through deletion or gene conversion whereby one of the copies substitutes its homeologous counterpart [18]. Gene conversion and the homogenization of complete chromosomes played a pivotal role in the evolution of the osmotolerant yeast species *Pichia sorbitophila* [19]. In total, two of its seven chromosome pairs consist of partly heterozygous, partly homozygous sections, whereas two chromosome pairs are completely homozygous. Gene conversion may eventually result in chromosomes consisting of sections of both parental origins as “mosaic genomes” [20]. However, mosaic genomes can also arise through recombination between chromosomes of the different parents, such as in the hybrid yeast *Zygosaccharomyces parabailii* [21].

The redundancy of having one or more additional homeolog copies for most genes facilitates functional diversification in allopolyploids [22]. Consequently, accelerated gene evolution is generally observed upon allopolyploidization [22,23]. Nevertheless, recent allopolyploidization events in the fungal genus *Trichosporon* resulted in a general deceleration of gene evolution [24]. Thus, allopolyploidization is not always followed by

accelerated gene evolution. Arguably, the environmental exposure upon allopolyploidization plays an pivotal role in the eventual speed and grade of gene diversification [25].

Allopolyploidization typically entails gene expression pattern alterations when parental genomes that evolved distinct transcriptional regulation merge [26]. Moreover, crosstalk between parental sub-genomes can lead to further gene expression alterations, leading to the emergence of novel expression patterns [27–29]. Nevertheless, in general, expression patterns are often conservatively inherited upon hybridization as the majority of allopolyploid genes are expressed similarly to their parental orthologs [30]. For instance, more than half of the genes in an allopolyploid strain of the fungal grass endophyte *Epichloë* retained their parental gene expression level [31].

Plant pathogens are often thought to evolve while being engaged in arms races with their hosts with pathogens evolving to evade host immunity while plant hosts attempt to intercept pathogen ingress [32,33]. Due to the increased adaptation potential, allopolyploidization has been proposed as a potent driver in pathogen evolution [34]. Allopolyploids often have different pathogenic traits than their parental lineages, such as higher virulence [35,36] and altered host ranges [37,38]. Within the fungal genus *Verticillium*, allodiploidization resulted in the emergence of the species *Verticillium longisporum* [37,39]. *V. longisporum* infects brassicaceous plants, whereas other *Verticillium* spp. generally do not typically colonize plants of this family, with the exception of *Arabidopsis thaliana* [37,40–42]. Similar to haploid *Verticillium* spp., *V. longisporum* is thought to have predominant asexual reproduction as a sexual cycle has never been described and populations are not outcrossing [39,43]. *V. longisporum* is sub-divided into three lineages, each representing a separate hybridization event [37]. The economically most important lineage A1/D1 originates from hybridization between *Verticillium* species A1 and D1 that have hitherto not been found in their haploid states. *V. longisporum* lineage A1/D1 is the main causal agent of *Verticillium*

stem striping on oilseed rape and a worldwide emerging pathogen [44,45]. Lineage A1/D1 can be further divided into two genetically distinct populations, which have been named ‘A1/D1 West’ and ‘A1/D1 East’ after their relative geographic occurrence in Europe [39]. Nevertheless, both populations originate from the same hybridization event [39]. Conceivably, upon or subsequent to the hybridization event, *V. longisporum* encountered extensive genetic and transcriptomic alterations that might have facilitated a shift towards brassicaceous hosts. Here, we studied the impact of allodiploidization on the evolution of *V. longisporum* by investigating genome, gene and transcriptomic plasticity.

## Results

### *V. longisporum* displays a mosaic genome structure

The genomes of two *V. longisporum* strains were analysed to investigate the impact of hybridization on the genome structure. Previously, *V. longisporum* strains VLB2 and VL20, belonging to ‘A1/D1 West’ and ‘A1/D1 East’, were sequenced with the PacBio RSII platform and assembled into genomes of 72.9 and 72.3 Mb in size, respectively [39]. These genome sizes exceed double the amount of the telomere-to-telomere sequenced *V. dahliae* strains JR2 (36.2 Mb) and VdLs17 (36.0 Mb) [46]. We used RepeatModeler (V1.0.8; Smit et al. 2015) in combination with RepeatMasker to determine that 14.28 and 13.90% of the *V. longisporum* strain VLB2 and VL20 genomes are composed of repeats, respectively (S1 Table). Intriguingly, this is more than double the repeat content as in *V. dahliae* strain JR2, for which 6.49% of the genome was annotated as repeat using the same methodology. The *V. longisporum* genomes were also screened for the fungal telomere-specific repeats (TAACCC/GGGTTA) to estimate the number of chromosomes. In total, 29 and 30 telomeric regions were found in the VLB2 and VL20 genomes, respectively, that were consistently situated at the end of sequence contigs, suggesting that *V. longisporum* contains at least 15

chromosomes (S1 Table). Six out of 45 and 4 out of 44 sequence contigs in strains VLB2 and VL20, respectively, were flanked on both ends by telomeric repeats and therefore likely represent complete chromosomes (S1 Table). For comparison, *V. dahliae* strains have 8 chromosomes [46].

In allodiploid organisms, parental origin determination is elementary to investigate genome evolution in the aftermath of hybridization. As species D1 is phylogenetically closer related, and consequently has a higher sequence identity, to *V. dahliae* than species A1, *V. longisporum* genomic regions were previously provisionally assigned to either species D1 or A1 [39]. Here, we determined the parental origin of *V. longisporum* genomic regions more precisely. The difference in phylogenetic distance of species A1 and D1 to *V. dahliae* caused that *V. longisporum* genome alignments to *V. dahliae* displayed a bimodal distribution with one peak at 93.1% and another peak at 98.4% sequence identity that represent the two parents with a dip at 96.0% (S1 Fig). In order to separate the two sub-genomes, regions with an average sequence identity to *V. dahliae* of <96% were assigned to species A1, whereas regions with an identity of ≥96% were assigned to species D1 (Fig 1). In this manner, 36.2 Mb of *V. longisporum* strain VLB2 was assigned to species A1 and 35.7 Mb to species D1. For *V. longisporum* strain VL20, 36.3 Mb was assigned to species A1 and 35.2 Mb to species D1. Only 1.0 and 0.8 Mb of strains VLB2 and VL20, respectively, could not be aligned to *V. dahliae* and thus remained unassigned.

To trace the chromosome sets of the original parents of the hybrid, the parental origin of individual contigs was determined. In total, 8 of the 10 largest contigs of *V. longisporum* strain VLB2 as well as strain VL20 consist of regions originating from both species A1 and species D1 (Fig 1). Thus, parental chromosome sets cannot be separated from one another as *V. longisporum* apparently evolved a mosaic genome structure in the aftermath of hybridization.



# **Genomic rearrangements are responsible for the mosaic genome**

Typically, a mosaic structure of a hybrid genome can originate from gene conversion or from chromosomal rearrangements between DNA strands of different parental origin [17]. To analyse the extent of gene conversion, genes were predicted for the *V. longisporum* strains VLB2 and VL20. To aid gene annotation with the BRAKER1 1.9 pipeline [47], ~2 Gb of filtered RNA-seq reads were generated from fungal cultures in liquid medium. In total, 19,123 and 18,784 genes were predicted for *V. longisporum* strains VLB2 and VL20 respectively, which is ~90% higher than the amount of genes that were predicted for *V. dahliae* strain JR2 using the same approach (9,909 genes) (S1 Table). As to be expected, the divergence of species A1 and D1 could also been observed at the gene level based on sequence identity and GC-content (Fig 1; S1 Fig). In total, 9,531 and 9,402 genes were assigned to the species A1 sub-genome of the strains VLB2 and VL20, respectively, whereas the number of genes in the species D1 sub-genomes was 9,468 and 9,243 for these strains, respectively (S1 Table). Thus, the amount of genes is similar in the two sub-genomes for both *V. longisporum* strains and similar to the gene number identified in *V. dahliae* strain JR2. Over 80% of the *V. longisporum* genes are present in two copies whereas almost all genes (97-98%) are present in one copy within each of the *V. longisporum* sub-genomes (S2 Fig). Moreover, of the 7,620 genes that are present in two copies in VLB2 and VL20, only 5 genes were found to be highly similar (<1% nucleotide sequence diversity) in VLB2, whereas the corresponding gene pair in VL20 was more diverse (>1%) (Fig 2A). In *V. longisporum* strain VL20, no highly similar copies were found that are more divergent in VLB2. Collectively, these findings indicate that the two copies of most genes present in the *V. longisporum* are homeologs and that gene conversion only played a minor role during evolution of the mosaic genome.

Considering that gene conversion played a minor role during genome evolution, the mosaic genome structure of *V. longisporum* likely originated from rearrangements between homeologous chromosomes. To identify the location of genomic rearrangements, the genome of *V. longisporum* strain VLB2 was aligned to that of strain VL20 (Fig 2B). Extensive chromosomal rearrangements occurred between the two *V. longisporum* strains, as we observed 87 putative syntenic breaks. In order to confirm these breaks, long sequencing reads of VLB2 were aligned to the VL20 genome assembly to assess if synteny breaks were supported by read mapping (S3 Fig). In total, 60 synteny breaks could be confirmed by read mapping. As genomic rearrangements are often associated with repeat-rich genome regions [48], the synteny break points were tested for their association to these regions. In total, 34 of the 60 (57%) confirmed synteny break points were flanked by repeats, which is significantly more than expected from random sampling (mean = 18.5%,  $\sigma$  = 0.05%) (S4 Fig). In conclusion, it appears that chromosomal rearrangement, rather than gene conversion, is the main driver underlying the mosaic structure of the *V. longisporum* genome.

### ***V. longisporum* lost heterozygosity through deletions**

In each of the *V. longisporum* isolates, 17% of the genes occur only in a single copy. Although gene conversion played a minor role in the aftermath of hybridization, loss of heterozygosity may occur through gene loss or, alternatively, single-copy genes may originate from parent-specific contributions. However, as 12% of the singly copy genes in strain VLB2 are present in two copies in strain VL20, and 16% of the single copy genes in VL20 are present in two copies in VLB2, gene deletion seems to be an on-going process in *V. longisporum* evolution since both strains are derived from the same hybridization event [39]. Of the genes that were lost in the VLB2 divergence from VL20, 52% resided in the species A1 sub-genome, whereas 47% in the D1 sub-genome (1% remained unassigned). For VL20,

49% and 50% of these lost genes resided in the A1 and D1 sub-genome, respectively. Thus, gene loss occurs evenly across the two sub-genomes. We next determined the fraction of lost genes that encode secreted proteins as pathogen secretomes play pivotal roles in establishing symbioses with plant hosts [49]. In total, 12.9% and 8.7% of the genes that encode secreted proteins were lost in the divergence of VLB2 and VL20, respectively. This is a significant enrichment for strain VLB2, where genome-wide 8.9% of the genes encode secreted proteins (Fisher's exact test,  $P = 0.009$ ) (S1 Table). Nevertheless, this enrichment is not found for strain VL20 of which 9.0% of the genes encode secreted proteins (Fisher's exact test,  $P = 0.45$ ) (S1 Table). Nonetheless, in general, *V. longisporum* strains VLB2 and VL20 contain 1.91 and 1.90 times the number of genes encoding secreted proteins compared to *V. dahliae* JR2 with similar contributions of the species A1 and D1 sub-genomes (S1 Table). This indicates that, although gene loss occurs, it hitherto impacted the secretome of *V. longisporum* only to a limited extent.

### Global acceleration of gene evolution upon allodiploidization

To investigate the evolution of genes subsequent to the allodiploidization event, we determined their rates of non-synonymous ( $Ka$ ) and synonymous ( $Ks$ ) substitutions. Substitution rates were determined for so-called best-reciprocal orthologs, which are genes that are present in a single copy in all *Verticillium* species (Fig 3A) and thus, sub-genomes A1 and D1 of *V. longisporum* were considered separately. In total, 5,342 and 5,369 orthologous groups could be constructed using *V. longisporum* strain VLB2 and VL20, respectively. Consequently, for every orthologous group,  $Ka/Ks$  ratios were determined for every branch of the *Verticillium* phylogeny leading to an extant species and consequently compared with the  $Ka/Ks$  ratio obtained for the *V. dahliae* branch. In general, genes in clade Flavexudans spp. displayed higher  $Ka/Ks$  ratios than clade Flavnonexudans spp. (Fig 3; S5 Fig). *V. nubilum* and

*V. albo-atrum* genes displayed the lowest  $Ka/Ks$  ratios of all *Verticillium* spp., which correlates with their relatively long evolutionary history without divergence of known sister species (Fig 3; S5 Fig). Of all *Verticillium* spp., *V. longisporum* sub-genome D1 was the only species of which genes displayed significantly higher  $Ka/Ks$  ratios than *V. dahliae* (Wilcoxon rank-sum test,  $P = 9.43\text{e-}12$ , VLB2 based). Thus, genes of the *V. longisporum* sub-genome D1 generally evolve faster than genes of other haploid *Verticillium* spp. In contrast, genes of the other *V. longisporum* sub-genome, A1, generally displayed lower  $Ka/Ks$  ratios than *V. dahliae* orthologs (Wilcoxon rank-sum test,  $P < 2.2\text{e-}16$ , VLB2 based). However, the absence of a phylogenetically closely related A1 sister species hampers the determination of putative differences in gene diversification rate before and after hybridization as  $Ka/Ks$  ratios can vary considerably between genes of haploid *Verticillium* spp. For instance, *V. longisporum* sub-genome A1 displays higher evolutionary speed, expressed by  $Ka/Ks$ , than *V. alfalfae* (Wilcoxon rank-sum test,  $P = 3.94\text{e-}14$ , VLB2 based) and a similar evolutionary speed to *V. nonalfalfae* (Wilcoxon rank-sum test,  $P = 0.09$ , VLB2 based), species that have the same last common ancestor with A1 as *V. dahliae* (Fig 3A).

To find evidence for accelerated evolution in both *V. longisporum* sub-genomes, we determined the number of genes under positive selection in every *Verticillium* (sub-)genome using the above formed orthologous groups. Genes under positive selection were determined based on a Z-test and varied considerably from 209 in the *V. longisporum* sub-genome A1 to 3 in *V. tricornis* (S6 Fig). Intriguingly, the *V. longisporum* sub-genomes A1 and D1 have the highest number of genes under positive selection (128 genes for species D1). The genomes *V. dahliae* and *V. zaregansianum* contain a considerable number of genes under positive selection; 103 and 99 respectively. To investigate whether particular functional gene properties are associated with genes under positive selection, the fractions of genes that encode secreted proteins were determined (S6 Fig). These fractions were not higher in the *V.*

*longisporum* sub-genomes than in *V. dahliae* and *V. zaregansianum*. Furthermore, no major differences in Clusters of Orthologous Group (COG) functional categories could be observed for genes under positive selection between sub-genome A1, sub-genome D1, *V. dahliae* and *V. zaregansianum* (S7 Fig). Thus, we conclude that *V. longisporum* genes globally diverge faster than genes of related haploid *Verticillium* spp.

## **Expression pattern homogenization in the hybridization aftermath**

To investigate the impact of allodiploidization on gene expression patterns, the expression of *V. longisporum* genes was compared with *V. dahliae* orthologs of isolates grown in culture medium. To this end, expression of single copy *V. dahliae* genes was compared with *V. longisporum* orthologs that are present in two copies: one in the species A1 sub-genome and one in the species D1 sub-genome. In total, 7,469 and 7,411 of these expressed gene clusters were found for *V. longisporum* strain VLB2 and VL20, respectively. Reads were mapped to the predicted *V. longisporum* genes of which 51% and 50% mapped to species A1 homeologs and 49% and 50% to the species D1 homeologs, for strains VLB2 and VL20, respectively, and thus we observed no general dominance in expression for one of the sub-genomes. Over 60% of the *V. dahliae* genes are not differentially expressed compared to A1 and D1 orthologs, indicating that the majority of the genes did not evolve differential expression patterns (Fig 4). In total, 29.6% and 24.2% of the genes are differently expressed compared to *V. dahliae* orthologs in the species A1 and D1 sub-genomes, respectively (Fig 4, VLB2 based). The significantly higher fraction of differentially expressed A1 genes (Fisher's exact test,  $P = 4.3\text{e-}13$ ) corresponds to the more distant phylogenetic relationship of A1 with *V. dahliae* than of D1. Intriguingly, however, significantly less D1 genes (18.5%, VLB2 based) were differently expressed to A1 homeologs than to *V. dahliae* orthologs despite the larger phylogenetic distance between *Verticillium* species A1 and D1 (Fisher's exact test,  $P < 2.2\text{e-}$

16). In general, the expression pattern of *V. longisporum* A1 and D1 sub-genomes are more similar to each other ( $\rho = 0.90$  for VLB2) than the expression pattern of sub-genome D1 and *V. dahliae* ( $\rho = 0.86$  for VLB2) (Fig 5; S2 Table). This discrepancy in phylogenetic relationship and expression pattern similarities may indicate that the expression patterns of species A1 and D1 homogenized upon hybridization. Moreover, for *V. longisporum* strains VLB2 and VL20, homeolog expression patterns within the same strain ( $\rho = 0.90$  for VLB2) correlated more than A1 and D1 expression patterns of different strains ( $\rho = 0.88$  for VLB2 A1 and VL20 D1) (Fig 5; S2 Table). Thus, expression patterns of homeologs may have synchronized in the aftermath of hybridization.

### ***In planta* secretome homogenization between *V. longisporum* sub-genomes**

To assess potential gene expression differences upon host colonization, gene expression patterns of *V. longisporum* and *V. dahliae* orthologs were also investigated *in planta*. To this end, oilseed rape plants were inoculated with VLB2 and VL20, respectively. As observed previously, oilseed rape plants inoculated with VLB2 developed typical *Verticillium* symptoms including stunted plant growth and leaf chlorosis [50]. In contrast, oilseed rape plants inoculated with VL20 did not display any disease symptoms. Accordingly, VLB2 DNA could be detected in oilseed rape stems, whereas VL20 DNA remained under the detection limit. In addition, *A. thaliana* plants were inoculated with *V. dahliae* strain JR2, and *V. longisporum* strains VLB2 and VL20. However, only JR2 DNA could be detected in above-ground plant material. Consequently, total RNA sequencing was performed for oilseed rape plants inoculated with *V. longisporum* strain VLB2 and *A. thaliana* plants inoculated with *V. dahliae* strain JR2. In total, ~1.5 Gb of filtered RNA-seq reads were generated from the *Verticillium* inoculated plant material. Similar to *V. longisporum* grown in culture medium, 49% and 51% of the reads mapped to the A1 and D1 sub-genomes of *V. longisporum*. Thus,

also *in planta* there is no expression dominance of one of the *V. longisporum* sub-genomes. Furthermore, 16.4% and 15.1% of the *V. longisporum* genes were differently expressed from *V. dahliae* orthologs in sub-genome A1 and D1, respectively (Fig 6). Thus, in correspondence with *V. longisporum* grown in culture medium, a larger fraction of A1 orthologs was differently expressed to *V. dahliae* orthologs than D1 orthologs (Fisher's exact test,  $P = 0.04$ ).

To elucidate a putative association of gene expression differences between *V. longisporum* and *V. dahliae* with their distinct host ranges, the fraction of differently expressed genes that encode secreted proteins was determined. For *Verticillium* grown in culture medium, 16.5% of the differentially expressed genes between *V. longisporum* and *V. dahliae* encode secreted proteins, whereas this is only 5.3% for genes without differential expression (Fig 6A). This enrichment of genes encoding secreted proteins was also found for isolate VL20 (S8 Fig). Correspondingly, *V. longisporum* genes that were differently expressed from *V. dahliae* orthologs were enriched for Pfam domains associated with secretion and host colonization, such as *Hce2* (PF14856), a domain found in putative effectors with homology to *Cladosporium fulvum* effector Ecp2 (Stergiopoulos et al. 2012; S3 Table). Similarly, genes encoding secreted proteins were also significantly enriched for differentially expressed genes between *V. longisporum* and *V. dahliae* *in planta* (Fig 6B). However, the fraction of 9.7% was significantly less than 16.5% for *Verticillium* grown in culture medium (Fig 6B). Thus, despite the colonization of *V. longisporum* and *V. dahliae* on a different host species, the enrichment of genes encoding secreted proteins is lower for *Verticillium* grown *in planta* compared with culture medium.

To see how the different sub-genomes contribute to the enrichment of genes encoding secreted proteins, we compared gene expression patterns of *V. longisporum* sub-genomes. For *V. longisporum* grown in culture medium, 19.4% of the genes that are differentially expressed between the A1 and D1 homeologs encode secreted proteins, whereas this is 5.8% for



homeologs with similar expression levels (Fig 7). Thus, similar to *V. longisporum* and *V. dahliae* orthologs, differentially expressed homeologs are enriched for genes that encode secreted proteins. Intriguingly, 7.9% of the genes with differential homeolog expression *in planta* encode secreted proteins, which is a similar fraction as for homeologs without differential expression (8.4%; Fig 7). Thus, upon plant colonization, there is no enrichment of genes that encode secreted proteins for differentially expressed homeologs. This lack of enrichment may be due to increased expression differences *in planta* between homeologs that encode non-secreted proteins. Alternatively, expression levels of homeologs encoding secreted proteins may homogenize *in planta* (Fig 7). In total, 11.2% and 9.5% of the genes that are differently regulated *in planta* from culture medium encode secreted proteins in sub-genome A1 and D1, respectively (Fig 7). This is a significantly larger fraction than for genes without differential expression: 7.2% and 7.9% for sub-genomes A1 and D1, respectively. In sub-genome A1, this enrichment of genes encoding secreted proteins was both present for *in planta* up-regulated (11.6%, Fisher's exact test,  $P < 1.74\text{e-}05$ ) and down-regulated (10.9%, Fisher's exact test,  $P < 4.23\text{e-}05$ ) genes. In contrast, in sub-genome D1, the enrichment was present for *in planta* up-regulated genes (12.3%, Fisher's exact test,  $P < 2.27\text{e-}05$ ), but not for down-regulated genes (7.7%, Fisher's exact test,  $P = 0.91$ ). Thus, in general, genes encoding secreted proteins underwent relatively more frequently expression alterations upon plant colonization compared to genes that encode for non-secreted proteins. Consequently, the lack of enrichment *in planta* is caused by an increased homogenization of homeolog expression patterns of genes encoding secreted proteins. This homogenization is illustrated by the expression pattern of genes encoding secreted proteins with a pectate lyase Pfam domain (PF03211), which is associated with host cell-wall degradation (S9 Fig) [52]. In total, 5 genes (*Pect\_ly\_1*, *Pect\_ly\_2*, *Pect\_ly\_3*, *Pect\_ly\_4* and *Pect\_ly\_5*), with a pectate lyase domain were found with two homeologous copies in *V. longisporum* and all of them were predicted to



be secreted. There was no differential expression between the homeologs *in planta* for all 5 genes, whereas in culture medium the homeologs are differentially expressed for *Pect\_ly\_1*, *Pect\_ly\_4* and *Pect\_ly\_5*. Homogenization of homeolog expression was achieved through down-regulation for *Pec\_ly\_1*, as both homeologs were not expressed *in planta*. In contrast, similar levels of homeolog *in planta* expression were achieved for *Pect\_ly\_4* and *Pect\_ly\_5* by the relative increase in expression of the D1 and A1 homeolog, respectively.

## DISCUSSION

Hybridization is a powerful evolutionary mechanisms often leading to the emergence of new plant pathogens with distinct pathogenic features from their parents [34,53]. We demonstrate the genomic and transcriptomic plasticity of the allodiploid *V. longisporum* pathogen and illustrate its potential for divergent evolution. Firstly, the plastic nature of the *V. longisporum* genome is displayed by its mosaic structure (Fig 1). Mosaicism in *V. longisporum* is not driven by homogenization that played a negligible role in the aftermath of hybridization (Fig 2A). Rather, *V. longisporum* mosaic genome structure is caused by extensive genomic rearrangements after hybridization (Fig 2B). Genomic rearrangements are major drivers of evolution and facilitate adaptation to novel or changing environments [48]. Genomic rearrangements are not specific to the hybrid nature of *V. longisporum* as other *Verticillium* spp. similarly encountered extensive chromosomal reshuffling [54–56]. As expected, the majority of the synteny breaks between the genomes of *V. longisporum* strains VLB2 and VL20 reside in repeat-rich genome regions (S4 Fig) as, due to their abundance, repetitive sequences are more likely to act as a substrate for unfaithful repair of double-strand DNA breaks [48]. Nonetheless, in *V. longisporum*, 43% of the synteny breaks identified are not associated with repeat-rich regions. Conceivably, the presence of two genomes also provides homeologous sequences with sufficient identity to mediate unfaithful repair. Secondly, *V.*

400 *longisporum* genes globally display accelerated evolution in comparison to orthologs of non-  
 401 hybrid *Verticillium* spp. This is illustrated by the increased abundance of genes under positive  
 402 selection and the more divergent evolution of D1 genes in comparison to its sister species *V.*  
 403 *dahliae* (Figs 3; S5 and S6 Figs). The increased rate of divergence is likely a result of having  
 404 two homeologs of most genes as this redundancy gives leeway to functional diversification  
 405 [57]. Previously, 29 genes in *V. dahliae* were determined to evolve under positive selection,  
 406 whereas in this study more than three times the amount was found (S6 Fig) [54]. Here, we  
 407 obtained higher numbers as a higher *P*-value cut-off was used ( $P < 0.05$  and instead of  $P <$   
 408  $0.01$ ). Moreover, we calculated positive selection based on the nucleotide substitutions along  
 409 the *V. dahliae* species branch, whereas de Jonge et al. (2013) determined positive selection  
 410 based on intraspecific substitutions, which is expected to have lower *Ka/Ks* ratios for genes  
 411 under positive selection than when interspecific mutations are used [58]. Finally,  
 412 allodiploidization resulted in transcriptomic alterations even though the majority of the *V.*  
 413 *longisporum* genes was not differently expressed from *V. dahliae* orthologs (Fig 4). As  
 414 species A1 and D1 are hitherto unfound in their haploid state, *V. dahliae* was used for  
 415 expression pattern comparison as it only recently diverged from species D1 and therefore  
 416 likely resembles D1 gene expression [37]. Unfortunately, species A1 currently lacks a known  
 417 sister species that could be used in the gene expression comparison (Fig 3A). Despite the  
 418 absence of the *V. longisporum* parents, expression patterns between the A1 and D1 sub-  
 419 genomes seem to have homogenized upon hybridization as they show more resemblance than  
 420 the expression pattern between *V. dahliae* and species D1 (Fig 5; S2 Table). *V. longisporum*  
 421 genes that were differently expressed to *V. dahliae* orthologs are enriched for genes encoding  
 422 secreted proteins (Fig 6; S8 Fig). However, that enrichment is higher for *Verticillium* grown  
 423 in culture medium compared with *in planta* (Fig 6). This may be a consequence of the  
 424 disappearance of expression differences between the *V. longisporum* homeologs as

homeologs that encode secreted proteins homogenized their expression upon host colonization (Fig 7).

Whole-genome duplication events are usually followed by extensive gene loss, often leading to reversion to the original ploidy state [59]. However, the so-called ‘haploidization’ of *V. longisporum* has only proceeded to a limited extent, as 80% of the genes are present in two copies (S2 Fig), whereas the haploid *V. dahliae* genome contains only 1% of its genes in two copies. Thus, the *V. longisporum* genome displays the symptoms of a recent allodiploid, with gene loss being an on-going process that by now has only progressed marginally. However, the retention of both homeolog copies can also be evolutionary advantageous as the presence of an additional gene copy may facilitate functional diversification of *V. longisporum* genes in comparison to haploid *Verticillium* spp. (Fig 3; S5 and S6 Figs). Gene duplication is an important mechanism for plant pathogens, including *V. dahliae*, to evade host immunity [55,60,61]. The LS regions of *V. dahliae*, which are enriched for active transposable elements, are derived from segmental duplications [54,55]. However, instead of the specific duplication of LS regions, *V. longisporum* hybridization resulted in a whole-genome duplication likely resulting in the global acceleration of gene evolution as genes encoding secreted proteins or genes associated with niche colonization were not enriched in genes that evolve under positive selection (S6 and S7 Figs).

Expression divergence of a particular gene may evolve through mutations in regulatory sequences of the gene itself (cis effects), such as promoter elements, or alterations in other regulatory factors (trans effects), such as chromatin regulation [27,62]. Conceivably, the surprisingly higher correlation of the sub-genome D1 expression pattern with A1 than with *V. dahliae* may originate from the disappearance of differences in trans regulators between species A1 and D1 upon hybridization as in *V. longisporum* they reside in the same nuclear environment (Fig 5; S2 Table) [27]. Homogenization of expression patterns of

homeologs has been similarly observed in the fungal allopolyploid *Epichloë* Lp1 [31]. Furthermore, the enrichment in genes encoding secreted proteins for *V. longisporum* genes that are differently regulated upon infection indicates their importance for infection, as secreted proteins play important roles in pathogen-host interactions (Gupta et al. 2015; Fig 7). Upon plant infection, expression of homeologs encoding secreted proteins homogenized, illustrating gene expression crosstalk between the different sub-genomes of *V. longisporum* (Fig 7). Ratio changes between homeolog expressions also occurred in synthetic allopolyploid *Arabidopsis* upon cold stress treatment [63]. Many of these ratio alterations were related to stress responses. Thus, conceivably, alterations in homeolog expression ratios facilitate the adjustment of allopolyploids to different environmental conditions.

## Conclusion

Allodiploidization is an intrusive evolutionary mechanism that involves extensive alterations in genome, gene and transcriptome evolution. *V. longisporum* displays signatures of rapid diversifying evolution in the aftermath of hybridization, illustrated by extensive genomic rearrangements and accelerated gene evolution. Furthermore, the regulatory crosstalk between sub-genomes can adjust gene expression depending on the environment. Thus, in comparison to non-hybrid *Verticillium* spp., *V. longisporum* has a high adaptive potential that can contribute to host immunity evasion and to the further specialization towards brassicaceous plant hosts.

## Material and methods

### Genome analysis

Genome assemblies of the two *V. longisporum* strains (VLB2 and VL20) and *V. dahliae* strain JR2 were previously published [39,46]. Telomeric regions were determined based on the

475 fungal telomeric repeat pattern: TAACCC/GGGTTA (minimum three repetitions) [46].  
476 Furthermore, additional repeats were identified and characterized using RepeatModeler  
477 (v1.0.8). *De novo*-identified repeats were combined with the repeat library from RepBase  
478 (release 20170127) [64]. The genomic coordinates of the repeats were identified with  
479 RepeatMasker (v4.0.6). Homologous genes were identified by nucleotide BLAST (v2.2.31+).  
480 Here, only hits with a minimal coverage of 80% with each other were selected.

## 481 482 **RNA sequencing, gene annotation and function determination**

483 To obtain RNA-seq data for *Verticillium* grown in culture medium, isolates JR2, VLB2 and  
484 VL20 were grown for three days in potato dextrose broth (PDB) with three biological  
485 replicates for every isolate. To obtain RNA-seq data from *Verticillium* grown *in planta*, two-  
486 week-old plants of the susceptible oilseed rape cultivar ‘Quartz’ were inoculated by dipping  
487 the roots for 10 minutes in  $1 \times 10^6$  conidiospores  $\text{ml}^{-1}$  spore suspension of *V. longisporum*  
488 isolates VLB2 and VL20, respectively [50]. Similarly, three-week-old *A. thaliana* (Col-0)  
489 plants were inoculated with *V. dahliae* isolate JR2, VLB2 and VL20, respectively. After root  
490 inoculation, plants were grown in individual pots in a greenhouse under a cycle of 16 h of  
491 light and 8 h of darkness, with temperatures maintained between 20 and 22°C during the day  
492 and a minimum of 15°C overnight. Three pooled samples (10 plants per sample) of stem  
493 fragments (3 cm) and complete flowering stems were used for total RNA extraction for  
494 oilseed rape and *A. thaliana*, respectively. Total RNA was extracted based on TRIzol RNA  
495 extraction (Simms et al. 1993). cDNA synthesis, library preparation (TruSeq RNA-Seq short-  
496 insert library), and Illumina sequencing (single-end 50 bp) was performed at the Beijing  
497 Genome Institute (BGI, Hong Kong, China). In total, ~2 Gb and ~1.5 Gb of filtered reads  
498 were obtained for the *Verticillium* samples grown in culture medium and *in planta*,

respectively. RNAseq data were submitted to the SRA database under the accession number: SRP149060.

Using RNA-seq from the in liquid medium grown cultures, gene annotation was performed for JR2, VLB2 and VL20 with the BRAKER1 1.9 pipeline [47] using GeneMark-ET [65] and AUGUSTUS [66]. Predicted genes with internal stop codons were removed from the analysis. The secretome prediction was done using SignalP4 (v4.1) [67], TargetP (v1.1) [68], and TMHMM (v2.0) [69] as described previously [70]. Pfam function domains were predicted using InterProScan [71]. Subsequently, Pfam enrichments was determined using hypergeometric tests, and significance values were corrected using the Benjamini-Hochberg false discovery method [72]. Clusters of Orthologous Group (COG) categories were determined for protein sequences using EggNOG (v4.5.1) [73].

## Parental origin determination

Sub-genomes were divided based on the differences in sequence identities between species A1 and D1 with *V. dahliae*. *V. longisporum* genomes of VLB2 and VL20 were aligned to the complete genome assembly of *V. dahliae* JR2 using NUCmer, which is part of the MUMmer package v3.23 [46,74]. Here, only 1-to-1 alignments longer than 10 kb and with a minimum of 80% identity were retained. Subsequent alignments were concatenated if they aligned to the same contig with the same orientation and order as the reference genome. The average nucleotide identity was determined for every concatenated alignment and used to divide the genomes into sub-genome.

The parental origin determination based on sequence identities of the exonic regions of genes was performed by BLAST (v2.6.0+). Here, hits with a minimum subject and query coverage of 80% were used. Furthermore, similar to Louis et al. (2012), differences in GC-content between homologous genes present in two copies were calculated accordingly:

$$dGC_{\text{gene}} = \frac{2 * GC_{\text{gene}}}{GC_{\text{gene}} + GChomolog}$$

(1)

$GC_{\text{gene}} = \text{GC\% of gene}$

$GChomolog = \text{GC\% of homolog}$

$dGC_{\text{gene}} = \text{GC ratio from the mean GC\% value}$

## Gene conversion and genomic rearrangements

Genes occurring in multiple copy were identified using nucleotide BLAST (v2.6.0+) and the sequence identity between these genes was determined. Here, hits with a minimum subject and query coverage of 80% were used.

The VLB2 genome assembly was aligned to VL20 to identify synteny breaks using NUCmer, which is part of the MUMmer package v3.23 [74]. Subsequent alignments were concatenated if they aligned to the same contig with the same orientation and order as the reference genome. In order to confirm synteny breaks, filtered *V. longisporum* long sequencing reads of VLB2 [39] were aligned to the *V. longisporum* VL20 genome with the Burrows-Wheeler Aligner (BWA) [75] and further processed with the samtools package (v1.3.1) [76]. Synteny breaks were visualized using the R package Sushi [77] and the Integrative Genomics Viewer [78]. The association between breaks with repeats was tested through permutation. First, the fraction of synteny breaks flanked by repeats was determined. Here, synteny breaks were assigned to reside in a “repeat-rich” region if a 1 kb window around the break consisted for more than 10% of repeats. The *V. longisporum* VL20 genome assembly was divided into windows of 1 kb using BEDTools (v2.26.0). To estimate the significance of the synteny break/repeat association [79], 10,000 permutations were executed with the same amount of windows as there were synteny breaks to determine the random distribution of repeat-rich regions.



549

## 550 **Phylogenetic tree**

551 Following *Verticillium* strains were used as representatives for their species: *V. albo-atrum* =  
 552 PD747, *V. alfalfae* = PD683, *V. dahliae* = JR2, *V. isaacii* = PD660, *V. klebahnii* = PD401, *V.*  
 553 *nonalfalfae* = TAB2, *V. nubilum* = PD621, *V. tricorpus* = PD593 and *V. zaregansianum* =  
 554 PD739. The phylogenetic tree was constructed based on nucleotide sequences of the  
 555 Benchmarking Universal Single-Copy Orthologs (BUSCOs) of fungi present in all  
 556 *Verticillium* spp. and the out-group species *Sodiomyces alkalinus* [80]. To this end, previously  
 557 published *Verticillium* and *S. alkalinus* assemblies were used [39,46,56,81]. In total, 277  
 558 orthologous groups were aligned using mafft (v7.271) (default settings) [82,83]. Aligned  
 559 genes were then concatenated, and the phylogenetic tree was inferred using RAxML with the  
 560 GTRGAMMA substitution model (v8.2.0) [84]. The robustness of the inferred phylogeny was  
 561 assessed by 100 rapid bootstrap approximations.

562

## 563 **Gene divergence**

564 Previously published annotations of the haploid *Verticillium* spp. were used to compare the  
 565 evolutionary speed of orthologs [46,56]. The VESPA (v1.0b) software was used to automate  
 566 this process [85]. The coding sequences for each *Verticillium* spp. were filtered and  
 567 subsequently translated using the VESPA ‘clean’ and ‘translate’ function. Homologous genes  
 568 were retrieved by protein BLAST (v2.2.31+) querying a database consisting of all  
 569 *Verticillium* protein sequences. Here, only hits with a minimum coverage of 70% were used.  
 570 Homologous genes were grouped with the VESPA ‘best\_reciprocal\_group’ function. Only  
 571 homology groups that comprised a single representative for every *Verticillium* spp. were used  
 572 for further analysis. Protein sequences of each homology group were aligned with muscle  
 573 (v3.8.31) [86]. The aligned protein sequences of the homology groups were conversed to



nucleotide sequence by the VESPA ‘map\_alignments’ function. The alignments were used to calculate  $Ka/Ks$  for every branch of the species phylogeny using codeml module of PAML (v4.8) with the following parameters: F3X4 codon frequency model, wag.dat empirical amino acid substitution model and no molecular clock [87]. To this end, the previously obtained phylogenetic tree topology was used: (((((*V. klebahnii*, *V. isaacii*), *V. tricorpus*), *V. zaregamsianum*), *V. albo-atrum*), (((*V. dahliae*, species D1), (*V. alfalfae*, *V. nonalfalfae*)), species A1), *V. nubilum*). When comparing the evolutionary speed between *V. dahliae* genes and its orthologs, extreme values  $Ka/Ks$  were discarded from further analysis, i.e.  $Ka/Ks < 0.0001$  and  $Ka/Ks \geq 2$ . Significance of positive selection was tested using a Z-test [88] and Z-values  $> 1.65$  were considered significant with  $P < 0.05$ .

## Gene expression analysis

The RNA sequencing reads of the *Verticillium* strains VLB2, VL20 and JR2 were uniquely mapped to their previously assembled genomes using the Rsubread package in R [39,46,89,90]. To compare gene expression patterns, gene orthologs were retrieved by protein BLAST (v2.2.31+). Here, only hits with a minimum sequence identity of 70% and of coverage of 80% were used. Only genes in single copy in *V. dahliae* with two orthologs in *V. longisporum* of different parental origin (one A1 copy and one D1 copy) were used for comparative analysis. The comparative transcriptomic analysis was performed with the package edgeR in R (v3.4.3) [90–92]. Expression patterns were corrected for putative length differences between orthologous genes. Genes are considered differently expressed when  $P$ -value  $< 0.05$  with a log2-fold-change  $\geq 1$ .  $P$ -values were corrected for multiple comparisons according to Benjamini and Hochberg [72].

## Acknowledgements

The authors would like to thank the Marie Curie Actions program of the European Commission that financially supported the research of J.R.L.D. Work in the laboratories of B.P.H.J.T. and M.F.S is supported by the Research Council Earth and Life Sciences (ALW) of the Netherlands Organization of Scientific Research (NWO). The funders had no role in study design, data collection and analysis, decision to publish, or preparation of the manuscript. We thank Sander Y.A. Rodenburg for sharing bioinformatics scripts.

# References

1. Wolfe KH. Yesterday's polyploids and the mystery of diploidization. *Nat Rev Genet.* 2001;2: 333–41.
2. Jiao Y, Wickett NJ, Ayyampalayam S, Chanderbali AS, Landherr L, Ralph PE, et al. Ancestral polyploidy in seed plants and angiosperms. *Nature.* 2011;473: 97–100.
3. Van de Peer Y, Mizrachi E, Marchal K. The evolutionary significance of polyploidy. *Nat Rev Genet.* 2017;18:411-24.
4. Soltis DE, Albert VA, Leebens-Mack J, Bell CD, Paterson AH, Zheng C, et al. Polyploidy and angiosperm diversification. *Am J Bot.* 2009;96: 336–48.
5. Hoegg S, Brinkmann H, Taylor JS, Meyer A. Phylogenetic timing of the fish-specific genome duplication correlates with the diversification of teleost fish. *J Mol Evol.* 2004;59: 190–203.
6. te Beest M, Le Roux JJ, Richardson DM, Brysting AK, Suda J, Kubešová M, et al. The more the better? The role of polyploidy in facilitating plant invasions. *Ann Bot.* 2012;109: 19–45.
7. Lohaus R, Van de Peer Y. Of dups and dinos: evolution at the K/Pg boundary. *Curr Opin Plant Biol.* 2016;30: 62–9.
8. Vanneste K, Maere S, Van de Peer Y. Tangled up in two: a burst of genome duplications at the end of the Cretaceous and the consequences for plant evolution. *Philos Trans R Soc B Biol Sci.* 2014;369: 20130353.
9. Vanneste K, Baele G, Maere S, Van de Peer Y. Analysis of 41 plant genomes supports a wave of successful genome duplications in association with the Cretaceous-Paleogene boundary. *Genome Res.* 2014; 1334–47.
10. Barker MS, Arrigo N, Baniaga AE, Li Z, Levin DA. On the relative abundance of autopolyploids and allopolyploids. *New Phytol.* 2015;210: 391–8.

11. Campbell MA, Ganley ARD, Gabaldón T, Cox MP. The case of the missing ancient fungal polyploids. *Am Nat.* 2016;188: 602–14.
12. Marcet-Houben M, Gabaldón T. Beyond the whole-genome duplication: phylogenetic evidence for an ancient interspecies hybridization in the baker's yeast lineage. *PLOS Biol.* 2015;13: e1002220.
13. Peris D, Moriarty R V, Alexander WG, Baker E, Sylvester K, Sardi M, et al. Hybridization and adaptive evolution of diverse *Saccharomyces* species for cellulosic biofuel production. *Biotechnol Biofuels.* 2017;10: 78.
14. Gibson B, Liti G. *Saccharomyces pastorianus*: genomic insights inspiring innovation for industry. *Yeast.* 2015;32: 17–27.
15. Doyle JJ, Flagel LE, Paterson AH, Rapp RA, Soltis DE, Soltis PS, et al. Evolutionary genetics of genome merger and doubling in plants. *Annu Rev Genet.* 2008;42: 443–61.
16. Matute DR, Butler IA, Turissini DA, Coyne JA. A test of the snowball theory for the rate of evolution of hybrid incompatibilities. *Science.* 2010;329: 1518–21.
17. Mixão V, Gabaldón T. Hybridization and emergence of virulence in opportunistic human yeast pathogens. *Yeast.* 2017;35: 5–20.
18. McGrath CL, Gout JF, Johri P, Doak TG, Lynch M. Differential retention and divergent resolution of duplicate genes following whole-genome duplication. *Genome Res.* 2014;24: 1665–75.
19. Louis VL, Despons L, Friedrich A, Martin T, Durrens P, Casarégola S, et al. *Pichia sorbitophila*, an interspecies yeast hybrid, reveals early steps of genome resolution after polyploidization. *G3.* 2012;2: 299–311.
20. Stukenbrock EH, Christiansen FB, Hansen TT, Dutheil JY, Schierup MH. Fusion of two divergent fungal individuals led to the recent emergence of a unique widespread pathogen species. *Proc Natl Acad Sci USA.* 2012;109: 10954–9.

21. Ortiz-Merino RA, Kuanyshev N, Braun-Galleani S, Byrne KP, Porro D, Branduardi P, et al. Evolutionary restoration of fertility in an interspecies hybrid yeast, by whole-genome duplication after a failed mating-type switch. *PLOS Biol.* 2017;15: e2002128.
22. Kimura M, Ohta T. On some principles governing molecular evolution. *Proc Natl Acad Sci USA.* 1974;71: 2848–52.
23. Hellsten U, Khokha MK, Grammer TC, Harland RM, Richardson P, Rokhsar DS. Accelerated gene evolution and subfunctionalization in the pseudotetraploid frog *Xenopus laevis*. *BMC Biol.* 2007;5: 31.
24. Sriswasdi S, Takashima M, Manabe R, Ohkuma M, Sugita T, Iwasaki W. Global deceleration of gene evolution following recent genome hybridizations in fungi. *Genome Res.* 2016;26: 1081–90.
25. Schranz ME, Mohammadin S, Edger PP. Ancient whole genome duplications, novelty and diversification: the WGD Radiation Lag-Time Model. *Curr Opin Plant Biol.* 2012;15: 147–53.
26. Grover CE, Gallagher JP, Szadkowski EP, Yoo MJ, Flagel LE, Wendel JF. Homoeolog expression bias and expression level dominance in allopolyploids. *New Phytol.* 2012;196: 966–71.
27. Tirosh I, Reikhav S, Levy AA, Barkai N. A yeast hybrid provides insight into the evolution of gene expression regulation. *Science.* 2009;324: 659–662.
28. Adams KL, Cronn R, Percifield R, Wendel JF. Genes duplicated by polyploidy show unequal contributions to the transcriptome and organ-specific reciprocal silencing. *Proc Natl Acad Sci USA.* 2003;100: 4649–54.
29. Buggs RJA, Elliott NM, Zhang L, Koh J, Viccini LF, Soltis DE, et al. Tissue-specific silencing of homoeologs in natural populations of the recent allopolyploid *Tragopogon mirus*. *New Phytol.* 2010;186: 175–83.

30. Yoo M-J, Szadkowski E, Wendel JF. Homoeolog expression bias and expression level dominance in allopolyploid cotton. *Heredity*. 2013;110: 171–80.
31. Cox MP, Dong T, Shen G, Dalvi Y, Scott DB, Ganley ARD. An interspecific fungal hybrid reveals cross-kingdom rules for allopolyploid gene expression patterns. *PLoS Genet*. 2014;10: e1004180.
32. Cook DE, Mesarich CH, Thomma BPHJ. Understanding plant immunity as a surveillance system to detect invasion. *Annu Rev Phytopathol*. 2015;53: 541–63.
33. Jones JDG, Dangl JL. The plant immune system. *Nature*. 2006;444: 323–29.
34. Depotter JRL, Seidl MF, Wood TA, Thomma BPHJ. Interspecific hybridization impacts host range and pathogenicity of filamentous microbes. *Curr Opin Microbiol*. 2016;32: 7–13.
35. Husson C, Aguayo J, Revellin C, Frey P, Ioos R, Marçais B. Evidence for homoploid speciation in *Phytophthora alni* supports taxonomic reclassification in this species complex. *Fungal Genet Biol*. 2015;77: 12–21.
36. Brasier CM, Kirk SA. Comparative aggressiveness of standard and variant hybrid alder phytophthoras, *Phytophthora cambivora* and other *Phytophthora* species on bark of *Alnus*, *Quercus* and other woody hosts. *Plant Pathol*. 2001;50: 218–29.
37. Inderbitzin P, Davis RM, Bostock RM, Subbarao KV. The ascomycete *Verticillium longisporum* is a hybrid and a plant pathogen with an expanded host range. *PLoS One*. 2011;6: e18260.
38. Zeise K, von Tiedemann A. Host specialization among vegetative compatibility groups of *Verticillium dahliae* in relation to *Verticillium longisporum*. *J Phytopathol*. 2002;150: 112–119.
39. Depotter JRL, Seidl MF, van den Berg GCM, Thomma BPHJ, Wood TA. A distinct and genetically diverse lineage of the hybrid fungal pathogen *Verticillium longisporum*

- population causes stem striping in British oilseed rape. *Environ Microbiol.* 2017;19: 3997–4009.
40. Eynck C, Koopmann B, Grunewaldt-Stoecker G, Karlovsky P, von Tiedemann A. Differential interactions of *Verticillium longisporum* and *V. dahliae* with *Brassica napus* detected with molecular and histological techniques. *Eur J Plant Pathol.* 2007;118: 259–74.
  41. Ellendorff U, Fradin EF, de Jonge R, Thomma BPHJ. RNA silencing is required for *Arabidopsis* defence against *Verticillium* wilt disease. *J Exp Bot.* 2009;60: 591–602.
  42. Fradin EF, Abd-El-Hallem A, Masini L, van den Berg GCM, Joosten MHJ, Thomma BPHJ. Interfamily transfer of tomato *Ve1* mediates *Verticillium* resistance in *Arabidopsis*. *Plant Physiol.* 2011;156: 2255–65.
  43. Short DPG, Gurung S, Hu X, Inderbitzin P, Subbarao KV. Maintenance of sex-related genes and the co-occurrence of both mating types in *Verticillium dahliae*. *PLoS One.* 2014;9: e112145.
  44. Novakazi F, Inderbitzin P, Sandoya G, Hayes RJ, von Tiedemann A, Subbarao KV. The three lineages of the diploid hybrid *Verticillium longisporum* differ in virulence and pathogenicity. *Phytopathology.* 2015;105: 662–73.
  45. Depotter JRL, Deketelaere S, Inderbitzin P, von Tiedemann A, Höfte M, Subbarao KV, et al. *Verticillium longisporum* , the invisible threat to oilseed rape and other brassicaceous plant hosts. *Mol Plant Pathol.* 2016;17: 1004–16.
  46. Faino L, Seidl M, Datema E, van den Berg GCM, Janssen A, Wittenberg AHJ, et al. Single-molecule real-time sequencing combined with optical mapping yields completely finished fungal genome. *MBio.* 2015;6: e00936-15.
  47. Hoff KJ, Lange S, Lomsadze A, Borodovsky M, Stanke M. BRAKER1: unsupervised RNA-seq-based genome annotation with GeneMark-ET and AUGUSTUS.

- Bioinformatics. 2016;32: 767–9.
48. Seidl MF, Thomma BPHJ. Sex or no sex: evolutionary adaptation occurs regardless. BioEssays. 2014;36: 335–45.
49. Gupta R, Lee SE, Agrawal GK, Rakwal R, Park S, Wang Y, et al. Understanding the plant-pathogen interactions in the context of proteomics-generated apoplast proteins inventory. Front Plant Sci. 2015;6: 352.
50. Depotter JRL, Rodriguez-Moreno L, Thomma BPHJ, Wood TA. The emerging British *Verticillium longisporum* population consists of aggressive *Brassica* pathogens. Phytopathology. 2017;107: 1399–1405.
51. Stergiopoulos I, Kourmpetis YAI, Slot JC, Bakker FT, De Wit PJGM, Rokas A. In silico characterization and molecular evolutionary analysis of a novel superfamily of fungal effector proteins. Mol Biol Evol. 2012;29: 3371–84.
52. Marín-Rodríguez MC, Orchard J, Seymour GB. Pectate lyases, cell wall degradation and fruit softening. J Exp Bot. 2002;53: 2115–9.
53. Stukenbrock EH. The role of hybridization in the evolution and emergence of new fungal plant pathogens. Phytopathology. 2016;106: 104–12.
54. de Jonge R, Bolton MD, Kombrink A, van den Berg GCM, Yadeta KA, Thomma BPHJ. Extensive chromosomal reshuffling drives evolution of virulence in an asexual pathogen. Genome Res. 2013;23: 1271–82.
55. Faino L, Seidl MF, Shi-Kunne X, Pauper M, van den Berg GCM, Wittenberg AHJ, et al. Transposons passively and actively contribute to evolution of the two-speed genome of a fungal pathogen. Genome Res. 2016;26: 1091–100.
56. Shi-Kunne X, Faino L, van den Berg GCM, Thomma BPHJ, Seidl MF. Evolution within the fungal genus *Verticillium* is characterized by chromosomal rearrangements and gene losses. Environ Microbiol. 2018; 20:1362-73.



57. Lynch M, Conery JS. The evolutionary fate and consequences of duplicate genes. *Science*. 2001;290: 1151–5.
58. McDonald JH, Kreitman M. Adaptive protein evolution at the *Adh* locus in *Drosophila*. *Nature*. 1991;351: 652–4.
59. Maere S, De Bodt S, Raes J, Casneuf T, Van Montagu M, Kuiper M, et al. Modeling gene and genome duplications in eukaryotes. *Proc Natl Acad Sci USA*. 2005;102: 5454–9.
60. Dutheil JY, Mannhaupt G, Schweizer G, Sieber CMK, Münsterkötter M, Güldener U, et al. A tale of genome compartmentalization: the evolution of virulence clusters in smut fungi. *Genome Biol Evol*. 2016;8: 681–704.
61. Fouche S, Plissonneau C, Croll D. The birth and death of effectors in rapidly evolving filamentous pathogen genomes. *Curr Opin Microbiol*. 2018;46: 34–42.
62. Shi X, Ng DWK, Zhang C, Comai L, Ye W, Chen ZJ. Cis- and trans-regulatory divergence between progenitor species determines gene-expression novelty in *Arabidopsis* allopolyploids. *Nat Commun*. 2012;3: 950.
63. Akama S, Shimizu-Inatsugi R, Shimizu KK, Sese J. Genome-wide quantification of homeolog expression ratio revealed nonstochastic gene regulation in synthetic allopolyploid *Arabidopsis*. *Nucleic Acids Res*. 2014;42: e46.
64. Bao W, Kojima KK, Kohany O. Repbase Update, a database of repetitive elements in eukaryotic genomes. *Mob DNA*. 2015;6: 11.
65. Lomsadze A, Burns PD, Borodovsky M. Integration of mapped RNA-Seq reads into automatic training of eukaryotic gene finding algorithm. *Nucleic Acids Res*. 2014;42: e119.
66. Stanke M, Diekhans M, Baertsch R, Haussler D. Using native and syntenically mapped cDNA alignments to improve de novo gene finding. *Bioinformatics*. 2008;24: 637–44.

67. Petersen TN, Brunak S, von Heijne G, Nielsen H. SignalP 4.0: discriminating signal peptides from transmembrane regions. *Nat Methods*. 2011;8: 785–6.
68. Emanuelsson O, Nielsen H, Brunak S, von Heijne G. Predicting subcellular localization of proteins based on their N-terminal amino acid sequence. *J Mol Biol*. 2000;300: 1005–16.
69. Krogh A, Larsson B, von Heijne G, Sonnhammer EL. Predicting transmembrane protein topology with a hidden Markov model: Application to complete genomes. *J Mol Biol*. 2001;305: 567–80.
70. Seidl MF, Faino L, Shi-Kunne X, van den Berg GCM, Bolton MD, Thomma BPHJ. The genome of the saprophytic fungus *Verticillium tricorpus* reveals a complex effector repertoire resembling that of its pathogenic relatives. *Mol Plant-Microbe Interact*. 2015;28: 362–73.
71. Jones P, Binns D, Chang HY, Fraser M, Li W, McAnulla C, et al. InterProScan 5: genome-scale protein function classification. *Bioinformatics*. 2014;30: 1236–40.
72. Benjamini Y, Hochberg Y. Controlling the false discovery rate : a practical and powerful approach to multiple testing. *J R Stat Soc B*. 1995;57: 289–300.
73. Huerta-Cepas J, Szklarczyk D, Forslund K, Cook H, Heller D, Walter MC, et al. eggNOG 4.5: a hierarchical orthology framework with improved functional annotations for eukaryotic, prokaryotic and viral sequences. *Nucleic Acids Res*. 2016;44: D286–D293.
74. Kurtz S, Phillippy A, Delcher AL, Smoot M, Shumway M, Antonescu C, et al. Versatile and open software for comparing large genomes. *Genome Biol*. 2004;5: R12.
75. Li H. Aligning sequence reads, clone sequences and assembly contigs with BWA-MEM. 2013. Preprint. Available from: arXiv: 1303.3997. Cited 28 May 2018.
76. Li H, Handsaker B, Wysoker A, Fennell T, Ruan J, Homer N, et al. The Sequence

- Alignment/Map format and SAMtools. *Bioinformatics*. 2009;25: 2078–9.
77. Phanstiel DH, Boyle AP, Araya CL, Snyder MP. Sushi.R: flexible, quantitative and integrative genomic visualizations for publication-quality multi-panel figures. *Bioinformatics*. 2014;30: 2808–10.
78. Robinson JT, Thorvaldsdóttir H, Winckler W, Guttman M, Lander ES, Getz G, et al. Integrative Genomics Viewer. *Nat Biotechnol*. 2011;29: 24–6.
79. Quinlan AR, Hall IM. BEDTools: a flexible suite of utilities for comparing genomic features. *Bioinformatics*. 2010;26: 841–2.
80. Simão FA, Waterhouse RM, Ioannidis P, Kriventseva EV., Zdobnov EM. BUSCO: assessing genome assembly and annotation completeness with single-copy orthologs. *Bioinformatics*. 2015;31: 3210–2.
81. Grum-Grzhimaylo AA, Debets AJM, van Diepeningen AD, Georgieva ML, Bilanenko EN. *Sodiomyces alkalinus*, a new holomorphic alkaliphilic ascomycete within the Plectosphaerellaceae. *Persoonia*. 2013;31: 147–58.
82. Katoh K, Standley DM. MAFFT multiple sequence alignment software version 7: improvements in performance and usability. *Mol Biol Evol*. 2013;30: 772–80.
83. Katoh K, Misawa K, Kuma K, Miyata T. MAFFT: a novel method for rapid multiple sequence alignment based on fast Fourier transform. *Nucleic Acids Res*. 2002;30: 3059–66.
84. Stamatakis A. RAxML version 8: a tool for phylogenetic analysis and post-analysis of large phylogenies. *Bioinformatics*. 2014;30: 1312–13.
85. Webb AE, Walsh TA, O’Connell MJ. VESPA: Very large-scale Evolutionary and Selective Pressure Analyses. *PeerJ Comput Sci*. 2017;3: e118.
86. Edgar RC. MUSCLE: Multiple sequence alignment with high accuracy and high throughput. *Nucleic Acids Res*. 2004;32: 1792–7.

87. Yang Z. PAML 4: phylogenetic analysis by maximum likelihood. *Mol Biol Evol.* 2007;24: 1586–91.
88. Stukenbrock EH, Dutheil JY. Comparing fungal genomes: insight into functional and evolutionary processes. *Methods Mol Biol.* 2012;835: 531–48.
89. Liao Y, Smyth GK, Shi W. The Subread aligner: fast, accurate and scalable read mapping by seed-and-vote. *Nucleic Acids Res.* 2013;41: e108.
90. R Core Team. [cited 28 May 2018] R: A language and environment for statistical computing [Internet]. Vienna, Austria: R Foundation for Statistical Computing; 2015. Available from: <https://www.r-project.org/>
91. Robinson MD, McCarthy DJ, Smyth GK. edgeR: a Bioconductor package for differential expression analysis of digital gene expression data. *Bioinformatics.* 2010;26: 139–40.
92. McCarthy DJ, Chen Y, Smyth GK. Differential expression analysis of multifactor RNA-Seq experiments with respect to biological variation. *Nucleic Acids Res.* 2012;40: 4288–97.
93. Mccarthy DJ, Smyth GK. Testing significance relative to a fold-change threshold is a TREAT. *Bioinformatics.* 2009;25: 765–71.

# Supporting informations

**S1 Table. Comparison *V. longisporum* and *V. dahliae* genomes.**

**S2 Table. Expression pattern correlation of genes between *V. dahliae* and *V. longisporum* sub-genomes.** VD = *V. dahliae*, A1 = *V. longisporum* A1 sub-genome and D1 = *V. longisporum* D1 sub-genome. Correlations are calculated with the Spearman's rank correlation coefficient based on the count per million (CPM) values.

**S3 Table. Pfam domain enrichment for differentially expressed *V. longisporum* (expression A1 and D1 homeologs combined) and *V. dahliae* orthologs in culture medium**

**S1 Fig. Lines of evidence for the parental origin of *V. longisporum* genomic regions.** (A) Distribution of sequence identity of *V. longisporum* alignments to *V. dahliae*. (B) The distribution of the sequence identity between *V. longisporum* exonic regions of genes and their *V. dahliae* orthologs. (C) Distribution of sequence identity between exonic regions of *V. longisporum* homologs that are present in two copies. Strains VLB2 and JR2 were used for *V. longisporum* and *V. dahliae*, respectively.

**S2 Fig. Gene copy number distribution within *Verticillium* (sub-)genomes.** “(A1)” and “(D1)” represent species A1 and D1 sub-genomes, respectively, of the *V. longisporum* strains VLB2 and VL20. For *V. dahliae*, the strain JR2 was used.

**Fig S3: Synteny break confirmation by mapping *V. longisporum* VLB2 reads to the VL20 genome.** Red and blue bars represent forward and reverse aligned VLB2 reads to the VL20 genome. The dashed lines show the suggested position in synteny break through genome alignment. (A) In particular cases, read alignments did not confirm the break in synteny. (B) In other cases, breaks in synteny were confirmed as reads abruptly stopped and started on these genome positions. (C) Breaks were also considered truthful if regions showed overlap in repeat-rich regions where read overlap between adjacent genome regions is lacking.

**Fig S4: The association of synteny breaks with repetitive elements.** The black curve represents the fraction of 60 randomly chosen 1 kb windows in the *V. longisporum* VL20 that are repeat-rich, which has been permuted 10,000 times. The red line indicates the fraction of true breaks that lay in a 1 kb window enriched for repeats (57%).

**Fig S5: Gene evolutionary speed comparison between *Verticillium* species.**  $K_a/K_s$  ratios ( $\omega$ ) between *V. dahliae* and other *Verticillium* spp. were compared. (A) Blue branches in the phylogenetic tree represent *Verticillium* species with a haploid evolutionary history, whereas red branches represent species with an allodiploid phase in their evolutionary history. The median difference in evolutionary speed between *V. dahliae* and orthologs was calculated in addition to the standard deviation ( $\sigma$ ). (B) The distribution of these differences in evolutionary speed is depicted for species of the *Verticillium* clade Flavnonexudans. For the *Verticillium* species A1 and D1, *V. longisporum* strain VL20 was used.

**Fig S6: Genes under positive selection in *Verticillium* species.** Genes with one ortholog in every *Verticillium* spp. were tested for positive selection using a Z-test ( $P < 0.05$ ). # = number of genes under positive selection SP = number of genes encoding secreted proteins under positive selection.

**Fig S7: Relative abundance of Clusters of Orthologous Group (COG) categories for genes under positive selection.** Only genes were included were the COG category/categories could be determined. Genes under positive selection had a Z-value  $> 1.65$  ( $P < 0.05$ ). For the *Verticillium* species A1 and D1, *V. longisporum* strain VLB2 was used.

**Fig S8: Differential expression in *V. longisporum* VL20 in relation to genes encoding secreted proteins.** Differential expression is calculated for species A1, species D1 and *V. longisporum* (expression A1 and D1 homeologs combined) with *V. dahliae* orthologs. Pie charts show fraction of genes encoding secreted proteins of not-differentially and differentially expressed genes, respectively. Significance of the different distributions was calculated the Fisher's exact test (ns = not significant, \*\*\* =  $P < 0.001$ ).

**Fig S9: Expression comparison of genes with a pectate lyase domain (PF03211).** Gene expressions are depicted for species A1 and species D1 homeologs of *V. longisporum* cultured in liquid medium and upon oilseed rape colonization, respectively. Bars represent the mean gene expression and error bars represent the standard deviation. The significance of difference in gene expression was calculated using *t*-tests relative to a threshold (TREAT) [93]. Level of significance: ns = not significant and \*\*\* =  $P < 0.001$ .

## FIGURE CAPTIONS

**Fig 1. Determination of parental origin of *Verticillium longisporum* genome sections.** The ten largest contigs of the genome assemblies of *V. longisporum* strains VLB2 and VL20 are depicted. Lane 1: regions with a sequence identity of at least 96% were assigned to Species D1 (orange), whereas ones with lower sequence identity to Species A1 (purple). Lane 2: sequence identity of *V. longisporum* alignments to *V. dahliae*. Lane 3: Sequence identity between exonic regions of *V. longisporum* and *V. dahliae* orthologs. Lane 4: Difference in sequence identity in percent point (pp) between exonic regions of *V. longisporum* double-copy genes. Only gene pairs with an ortholog in *V. dahliae* are depicted. Alleles with a higher identity to *V. dahliae* are depicted as a positive pp difference, whereas the corresponding homolog as a negative pp difference. Lane 5: the relative difference in GC content (dGC) between genes in double copy. Lane 6: Read depth with non-overlapping windows of 10 kb. Data points of lanes 3-5 represent the average value of a window of eleven genes, which proceed with a step of one gene.



**Fig 2. The origin of the mosaic genome structure of *V. longisporum*.** (A) The contribution of gene conversion to *V. longisporum* genome evolution. Sequence identities between genes in copy, present in *V. longisporum* VLB2 and VL20, are depicted. Gene pairs that encountered gene conversion (purple dots in the red zones) have sequence divergence of more than one percent in one *V. longisporum* strain and less than one percent in the other strain. In other cases, pairs that differ less than one percent are depicted as a black dot, whereas a difference greater than one percent is depicted as a blue dot. (B) The contribution of genomic rearrangements to *V. longisporum* genome evolution. The ten largest contigs of the *V. longisporum* strains VLB2 (displayed on the right) and VL20 (displayed on the left) are depicted with complete chromosomes indicated by asterisks. Ribbons indicate syntenic genome regions between the two strains and contig colors indicate the parental origin similar to Fig 1 (purple = A1 and orange = D1). Regions without ribbons do not have homology to regions in the 10 largest contigs of the other isolate. Red bars on the contigs indicate synteny breaks that are confirmed by discontinuity in read alignment of VLB2 to the VL20 genome assembly (S3 Fig).

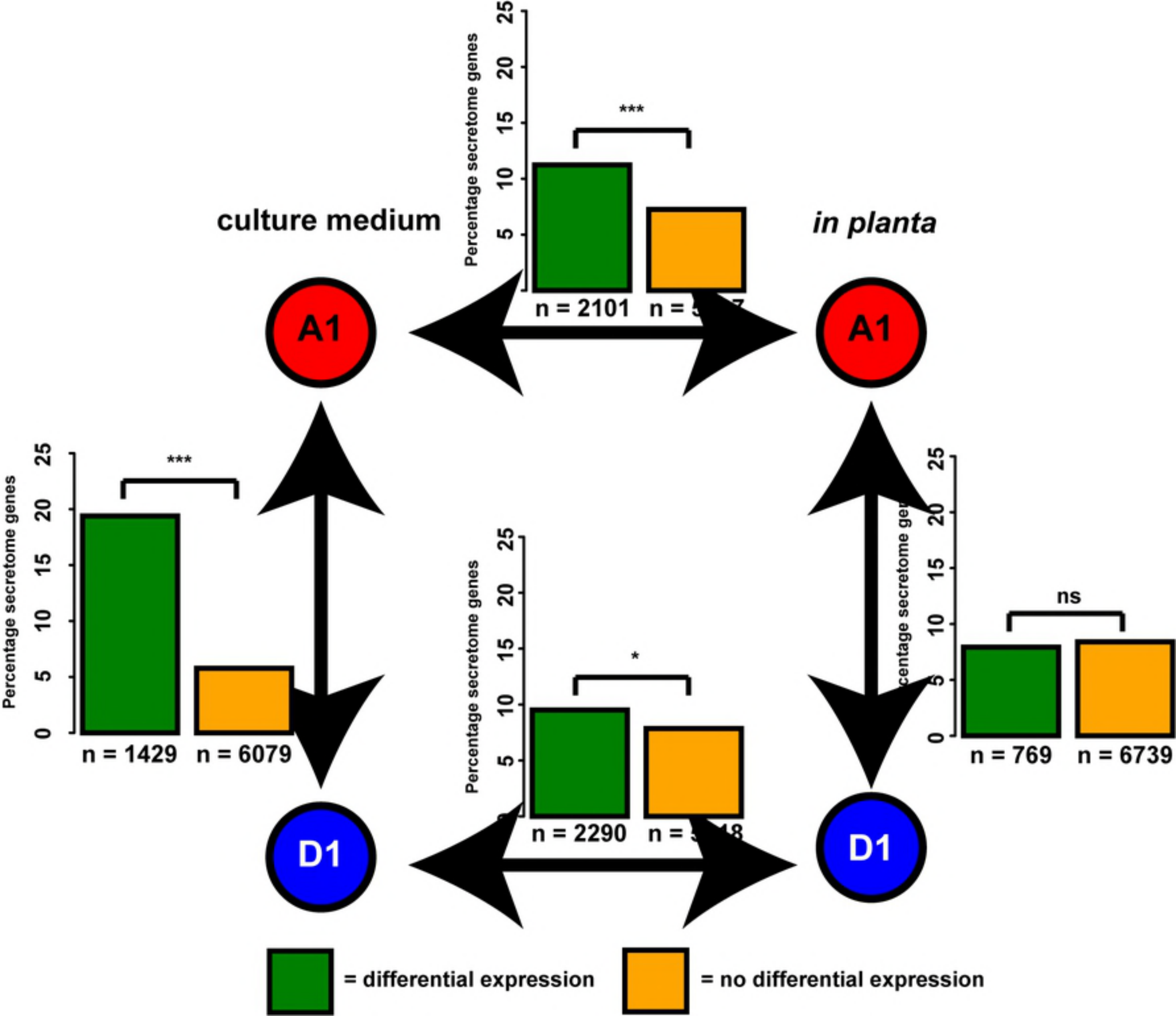
**Fig 3. Comparison of gene divergence between *Verticillium* species.**  $Ka/Ks$  ratios ( $\omega$ ) between *V. dahliae* and other *Verticillium* spp. were compared. (A) Blue branches in the phylogenetic tree represent *Verticillium* species with a haploid evolutionary history, whereas red branches represent species with an allodiploid phase in their evolutionary history. The median difference in evolutionary speed between *V. dahliae* and orthologs was calculated in addition to the standard deviation ( $\sigma$ ). (B) The distribution of these differences is depicted for species of the *Verticillium* clade Flavnonexudans. For the *Verticillium* species A1 and D1, *V. longisporum* strain VLB2 was used.

**Fig 4. Global comparison of expression between *V. longisporum* and *V. dahliae* orthologs.** Only genes with one copy in *V. dahliae* and two orthologs in the *V. longisporum* strains VLB2 and VL20 (one from sub-genome A1 and one from sub-genome D1) were considered.

**Fig 5. Expression pattern comparison between *V. longisporum* sub-genomes and *V. dahliae*.** Only genes with one copy in *V. dahliae* and two orthologs in the *V. longisporum* strains VLB2 and VL20 (one from sub-genome A1 and one from sub-genome D1) were considered. (A) Pairwise correlations between *Verticillium* expression patterns. Dot size and colour represent the Spearman's correlation coefficient ( $\rho$ ). (B) Relative expression (Z-scores) between *Verticillium* spp. VD = *V. dahliae*, A1 = *V. longisporum* A1 sub-genome and D1 = *V. longisporum* D1 sub-genome.

**Fig 6. Differential expression between *V. longisporum* and *V. dahliae* in relation to genes encoding secreted proteins.** Differential expression is calculated for species A1, species D1 and *V. longisporum* (cumulative expression A1 and D1 homeologs) with *V. dahliae* orthologs for isolates grown in (A) culture medium and (B) *in planta*. Pie charts show fraction of genes encoding secreted proteins of not-differentially and differentially expressed genes, respectively. Significance of the different distributions was calculated the Fisher's exact test (\*\*\*) =  $P < 0.001$ ).

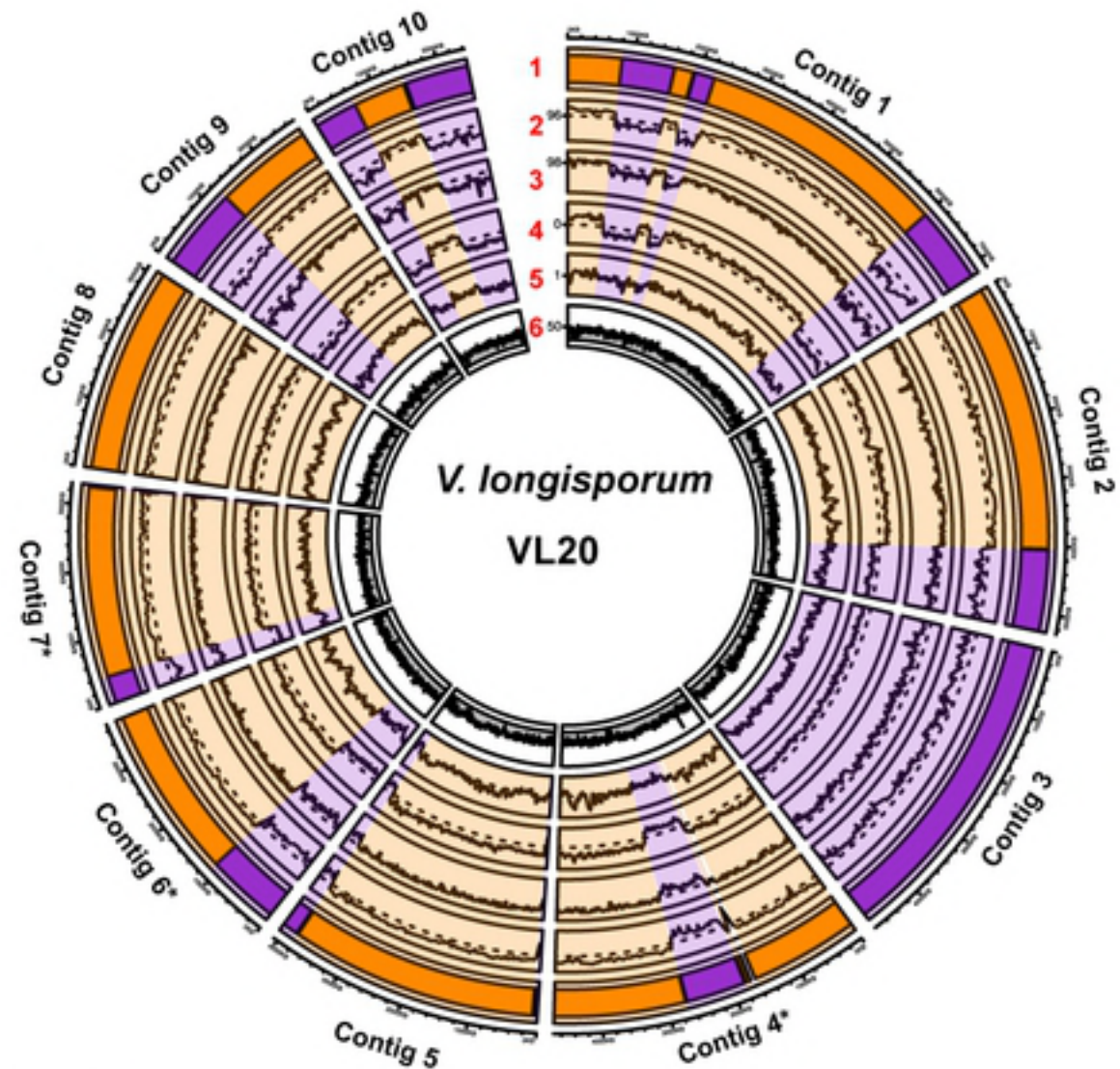
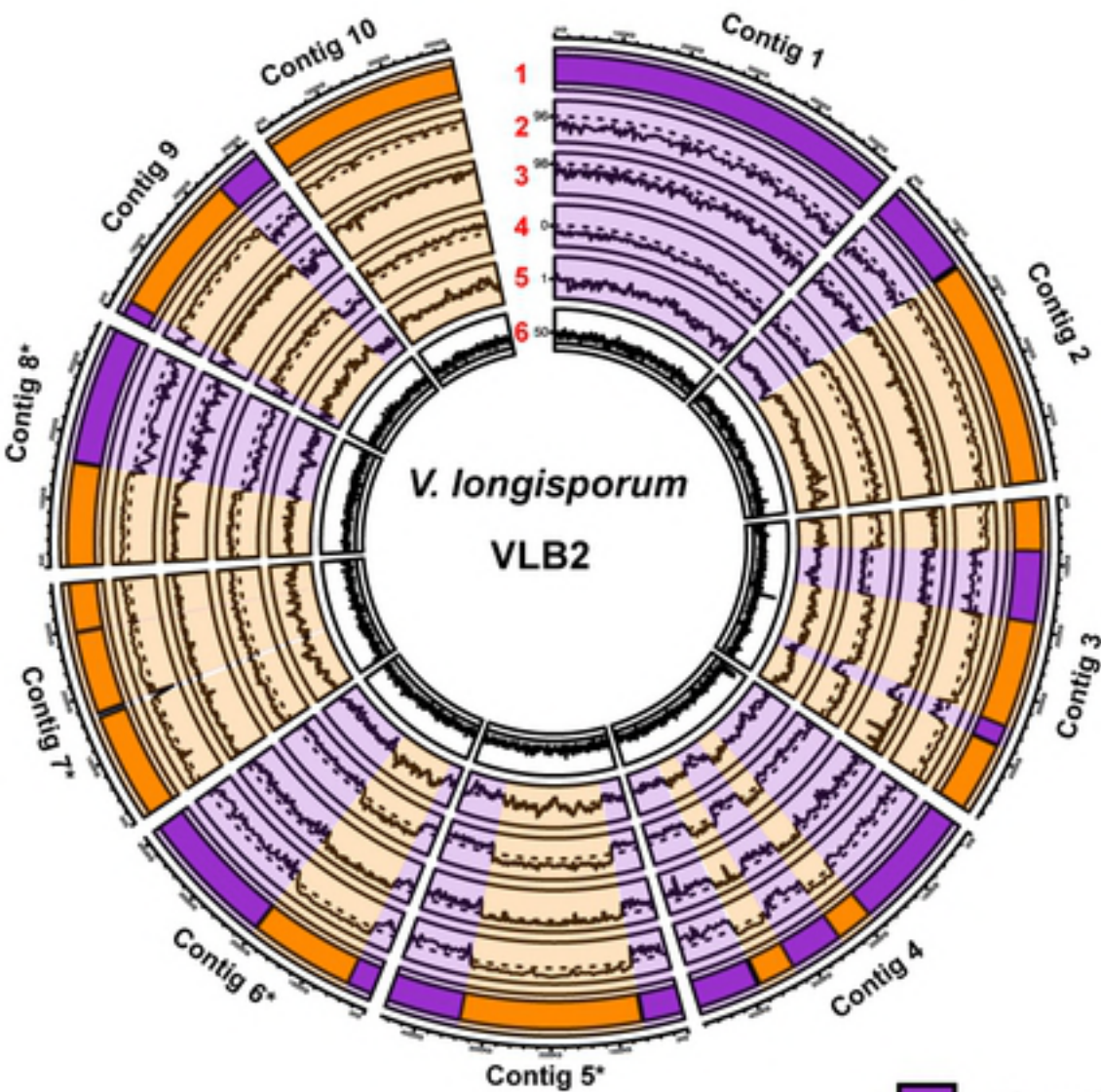
**Fig 7: Differential expression between *V. longisporum* sub-genomes in relation to genes encoding secreted proteins.** Gene expression of A1 and D1 homeologs were compared for *V. longisporum* grown in culture medium and *in planta*. Only genes were considered with one copy in *V. dahliae* and two corresponding copies in the *V. longisporum* strains VLB2 (one from sub-genome A1 and one from sub-genome D1). The number below the bar indicates the amount of differently and not differently expressed genes, respectively. Significance of the different distributions was calculated the Fisher's exact test (ns = not significant, \* =  $P < 0.05$ , \*\*\* =  $P < 0.001$ ).





# Lanes

- 1) Parental origin genome regions
- 2) Alignment sequence identity to *V. dahliae* (%)
- 3) Sequence identity to *V. dahliae* orthologs (%)
- 4) Sequence divergence between double-copy genes (pp)
- 5) Differential GC content between double-copy genes (dGC)
- 6) Read depth

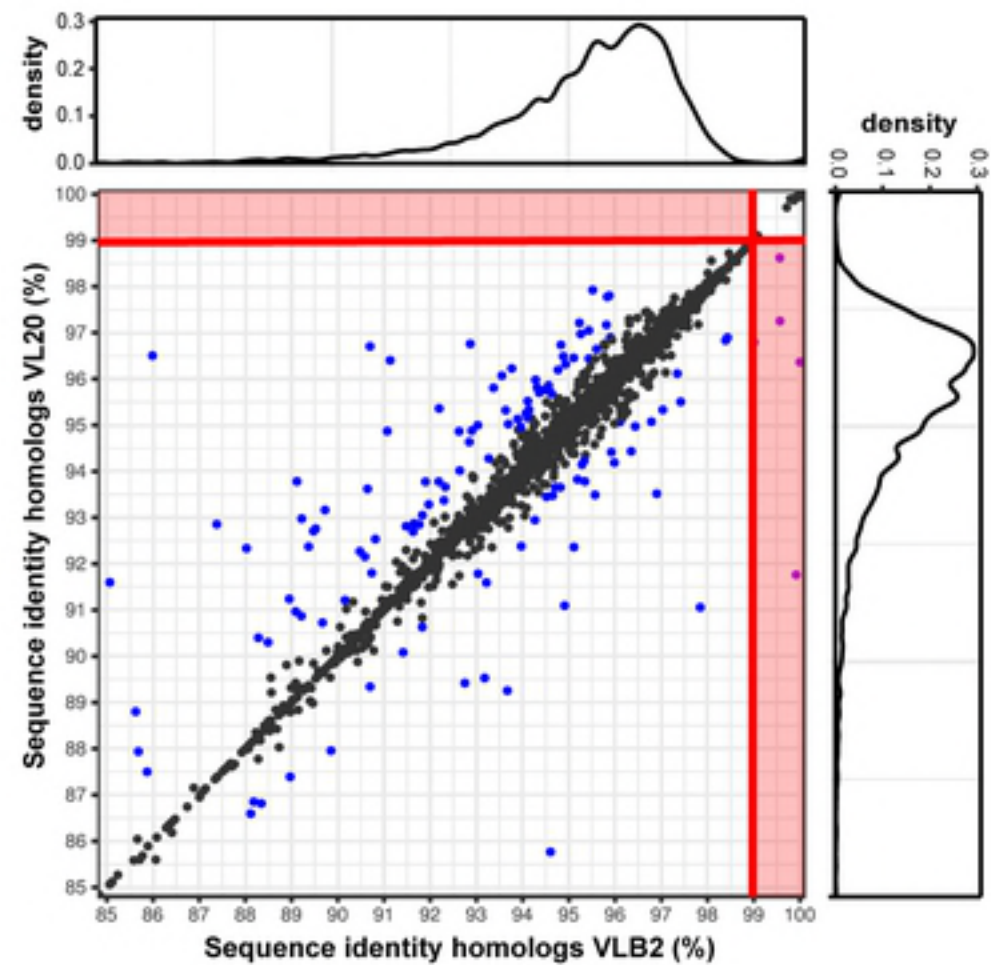


■ = Species A1 sub-genome

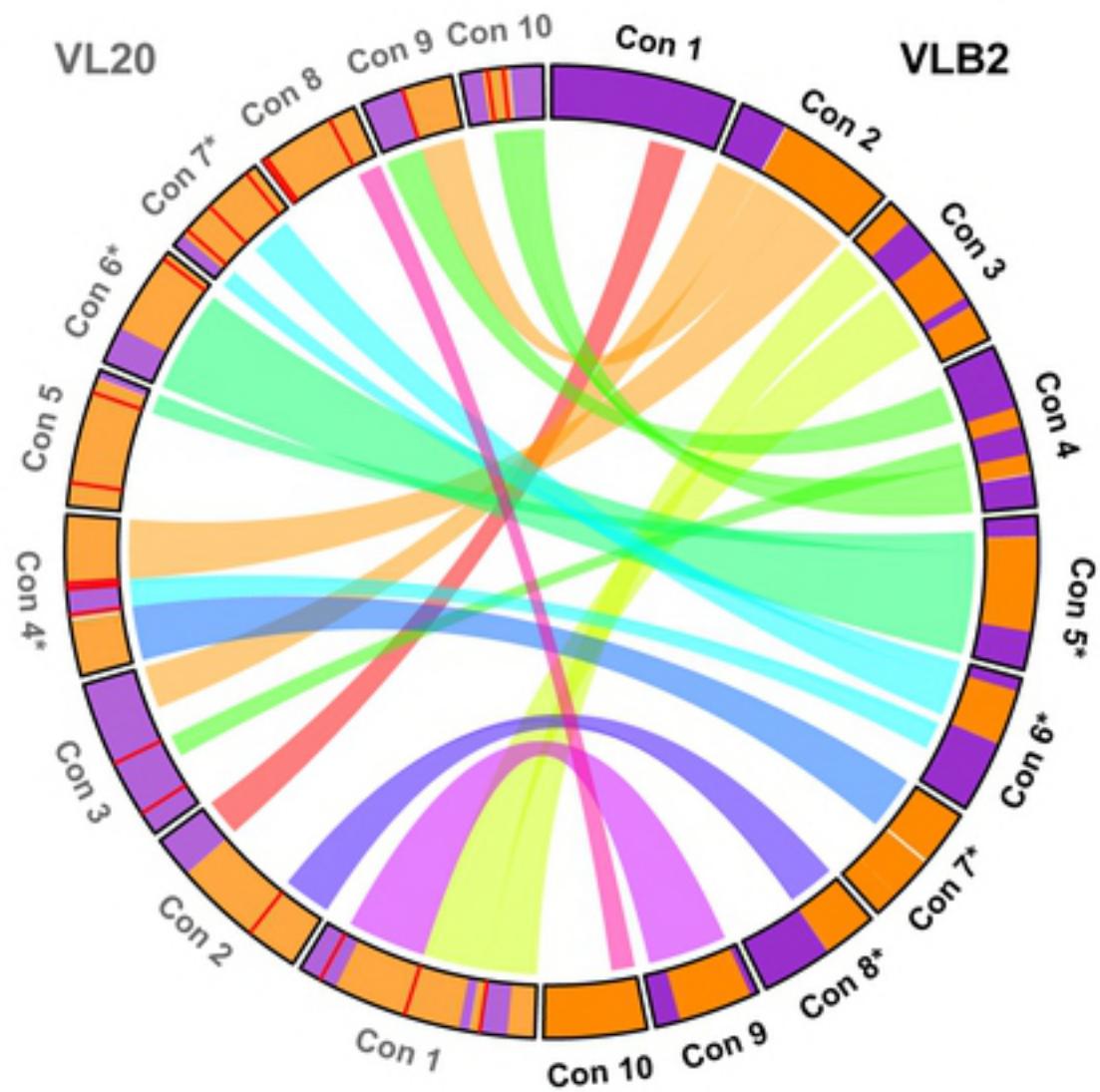
■ = Species D1 sub-genome

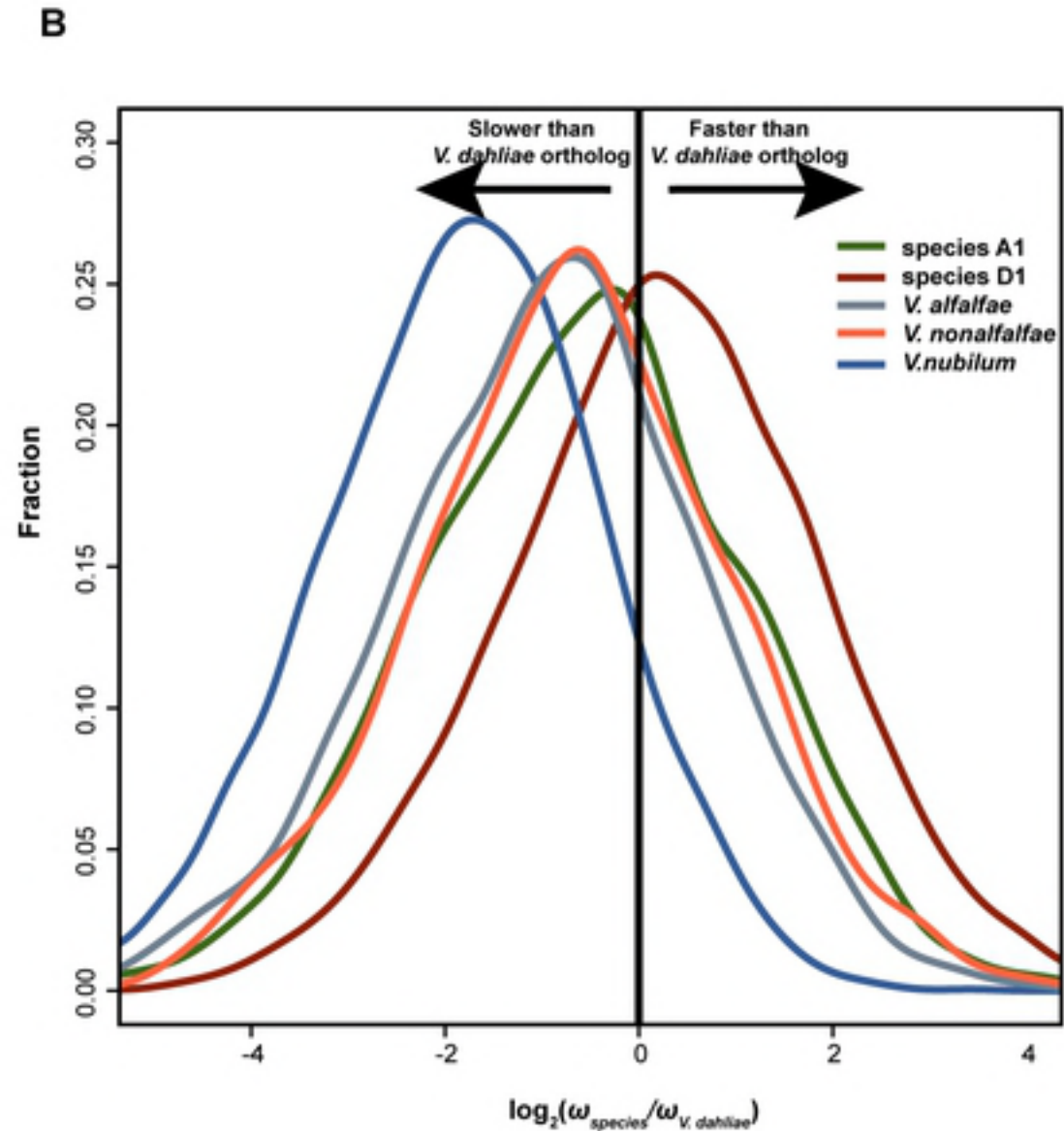
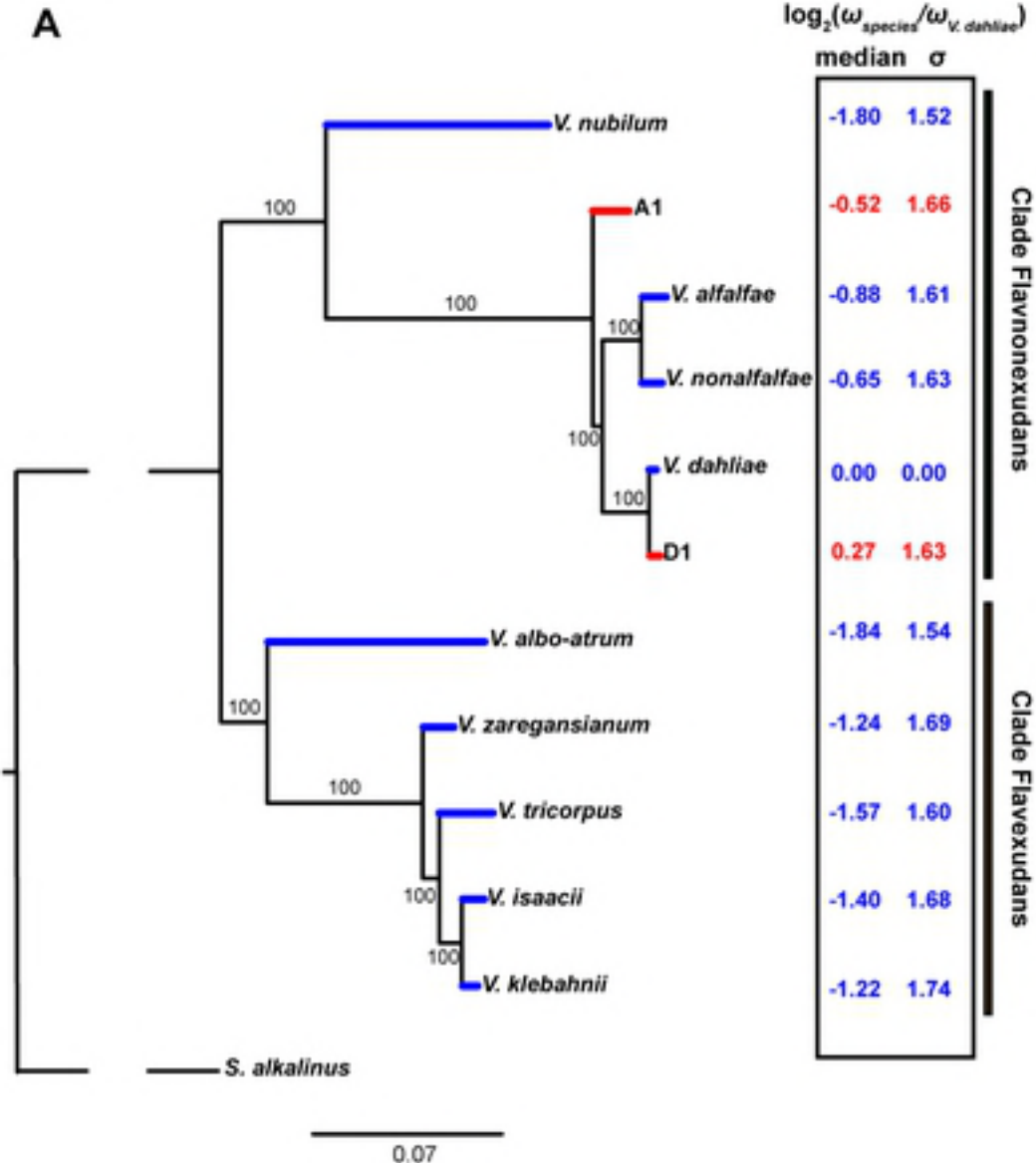


A




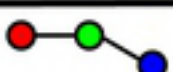







B



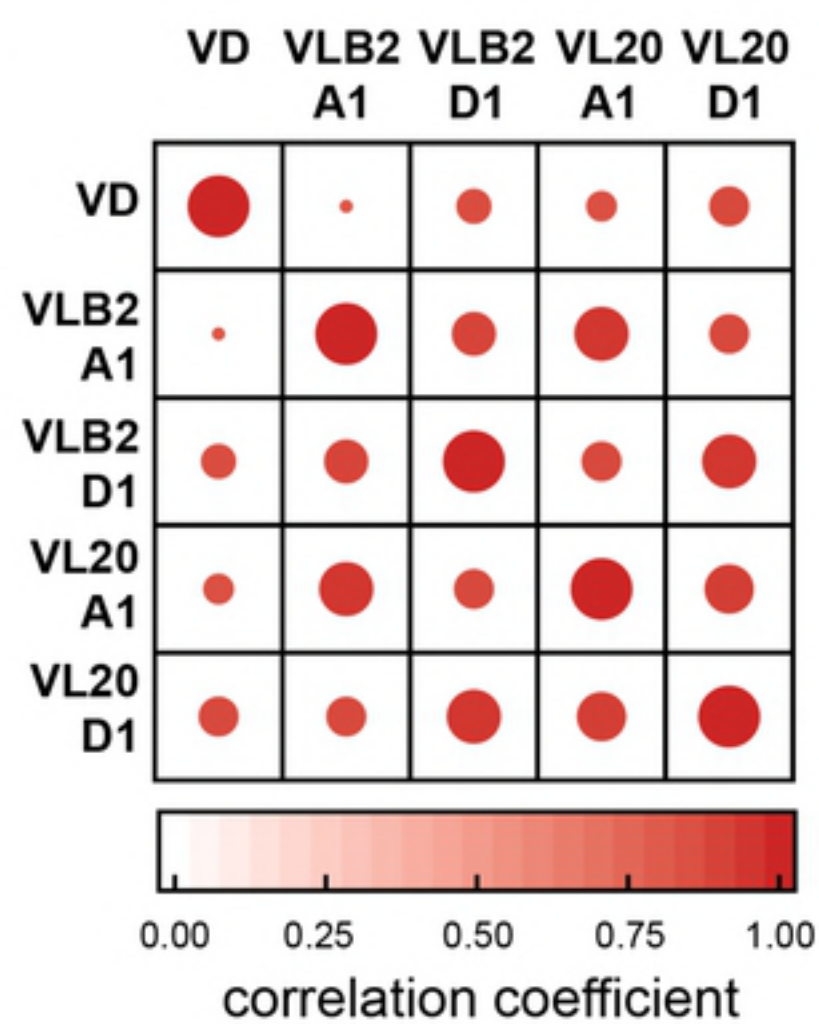




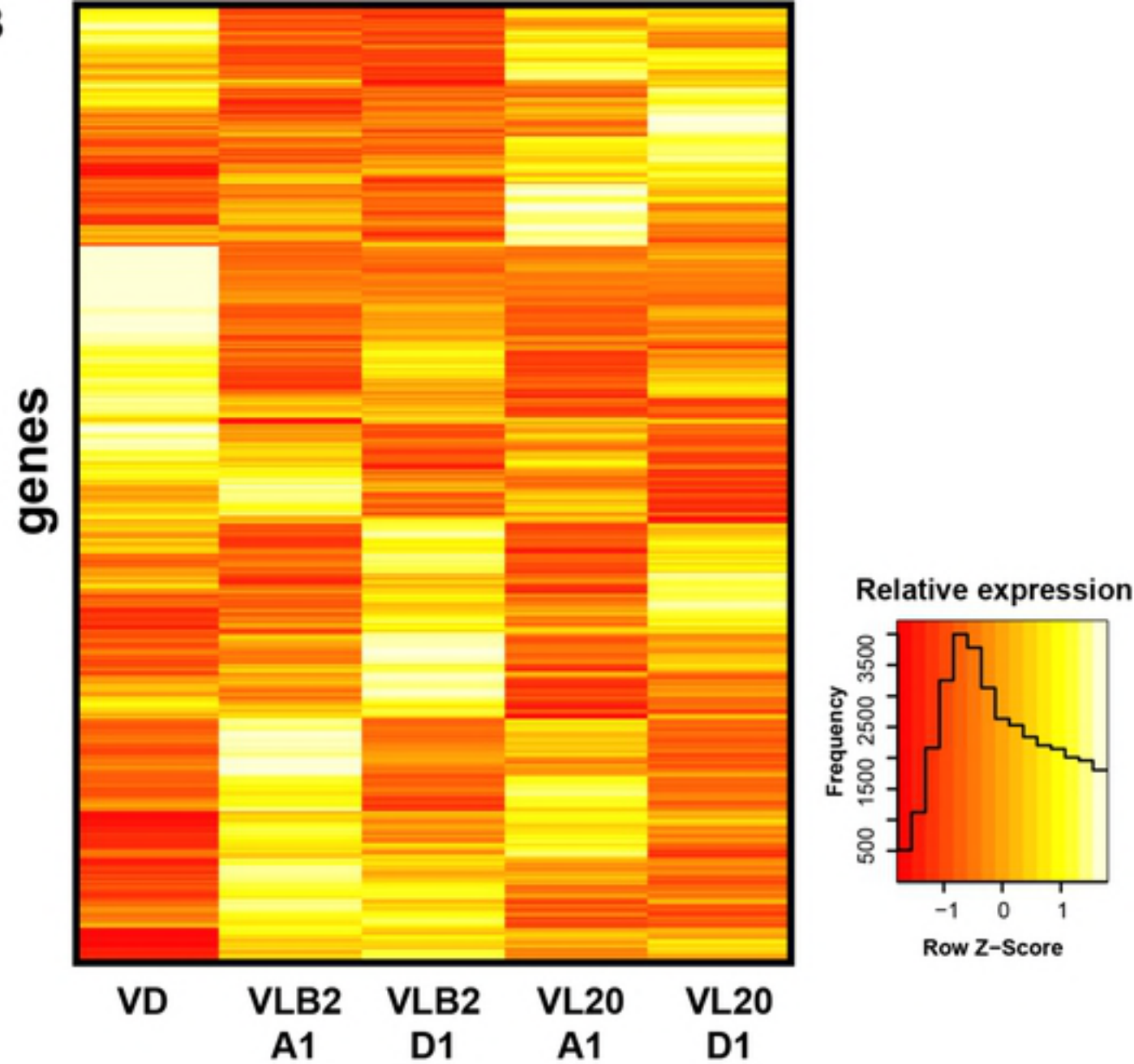
VLB2		VL20				VLB2		VL20	
776	692	One homeolog upregulated				290	277		
10.9%	9.7%					4.1%	3.9%		
						486	415		
						6.8%	5.8%		
790	761	One homeolog downregulated				301	277		
11.1%	10.7%					4.2%	3.9%		
						489	484		
						6.9%	6.8%		
82	40	Haploid intermediate expression				49	21		
1.2%	0.6%					0.7%	0.3%		
						33	19		
						0.5%	0.3%		
4416	4651	No differential expression							
62.1%	65.4%								
499	476	Both homeologs upregulated							
7.0%	6.7%								
550	493	Both homeologs downregulated							
7.7%	6.9%								



A



B



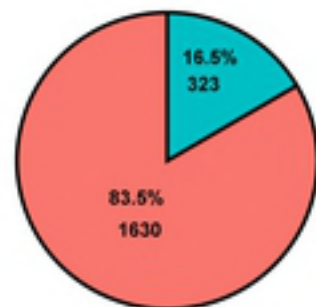
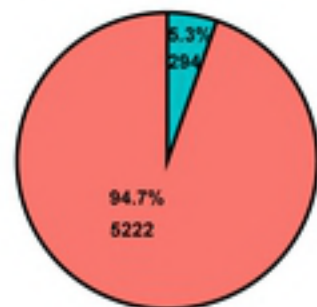
A

Culture medium

\*\*\*

No differential expression

Differential expression



= no secreted protein  
 = secreted protein

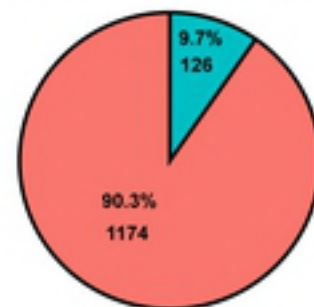
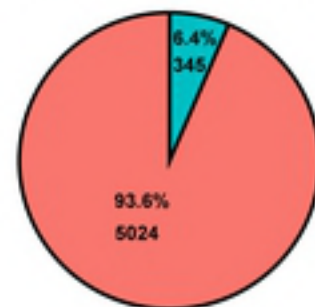
B

*In planta*

\*\*\*

No differential expression

Differential expression



\*\*\*

\*\*\*

species A1

No differential expression

Differential expression

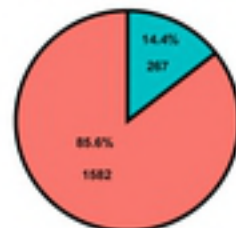


\*\*\*

species D1

No differential expression

Differential expression

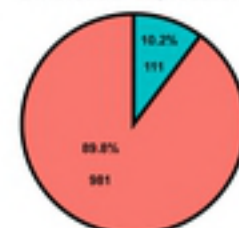


\*\*\*

species A1

No differential expression

Differential expression



\*\*\*

species D1

No differential expression

Differential expression

